

The Generalized Polarizabilities of the proton

Nikos Sparveris



Temple
University

SPIN 2018

Ferrara, Italy, September 2018

Supported by the DOE / NP award DE-SC0016577 and the NSF / PHY award 1305536

Proton Polarizabilities

Fundamental structure constants
(such as mass, size, shape, ...)

Response of internal structure
& dynamics to external EM field

Sensitive to the full excitation
spectrum of the nucleon

Accessed experimentally through
Compton Scattering processes

Virtual Compton Scattering:

Virtuality of photon gives access to the
Generalized Polarizabilities $\alpha_E(Q^2)$ & $\beta_M(Q^2)$ (+ 4 spin GPs)

→ mapping out the spatial distribution of
the polarization densities

Fourier transform of densities of electric charges and
magnetization of a nucleon deformed by an applied EM field

PDG

150 Baryon Summary Table

N BARYONS
($S = 0, I = 1/2$)

$p, N^+ = uud; n, N^0 = udd$

P

$$I(J^P) = \frac{1}{2}(\frac{1}{2}^+)$$

Mass $m = 1.00727646681 \pm 0.00000000009$ u

Mass $m = 938.272046 \pm 0.000021$ MeV [a]

$|m_p - m_{\bar{p}}|/m_p < 7 \times 10^{-10}$, CL = 90% [b]

$|\frac{q_p}{m_p}|/(\frac{q_p}{m_p}) = 0.9999999991 \pm 0.0000000009$

$|q_p + q_{\bar{p}}|/e < 7 \times 10^{-10}$, CL = 90% [b]

$|q_p + q_e|/e < 1 \times 10^{-21}$ [c]

Magnetic moment $\mu = 2.792847356 \pm 0.000000023 \mu_N$

$(\mu_p + \mu_{\bar{p}}) / \mu_p = (0 \pm 5) \times 10^{-6}$

Electric dipole moment $d < 0.54 \times 10^{-23}$ e cm

Electric polarizability $\alpha = (11.2 \pm 0.4) \times 10^{-4} \text{ fm}^3$

Magnetic polarizability $\beta = (2.5 \pm 0.4) \times 10^{-4} \text{ fm}^3$ ($S = 1.2$)

Charge radius, $e p$ Lamb shift = 0.84087 ± 0.00039 fm [d]

Charge radius, $e p$ CODATA value = 0.8775 ± 0.0051 fm [d]

Magnetic radius = 0.777 ± 0.016 fm

Mean life $\tau > 2.1 \times 10^{29}$ years, CL = 90% [e] ($p \rightarrow$ invisible mode)

Mean life $\tau > 10^{31}$ to 10^{33} years [e] (mode dependent)

Proton GPs

Intense experimental effort on $\alpha_E(Q^2)$ & $\beta_M(Q^2)$:

- currently facing a puzzle with respect to the electric GP
- new results are coming up
- new experiments are coming up

Spin polarizabilities:

- They have been measured in RCS (A2/MAMI): PRL 114, 112501 (2015)
- VCS: only one measurement (A1/MAMI) of a structure function that is a combination of the electric GP and two spin GPs

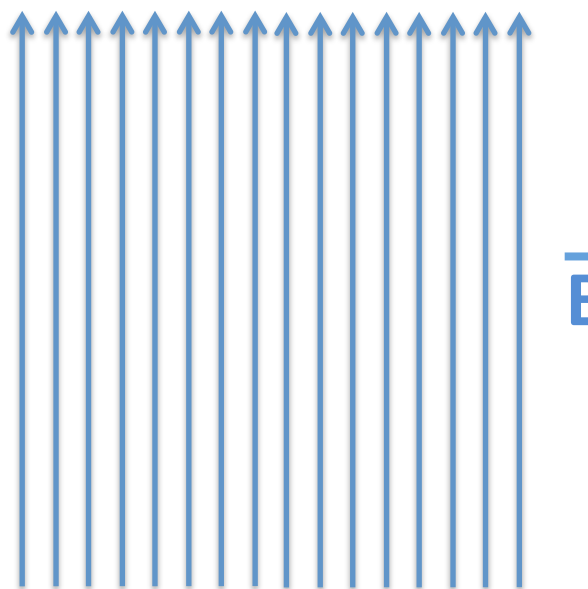
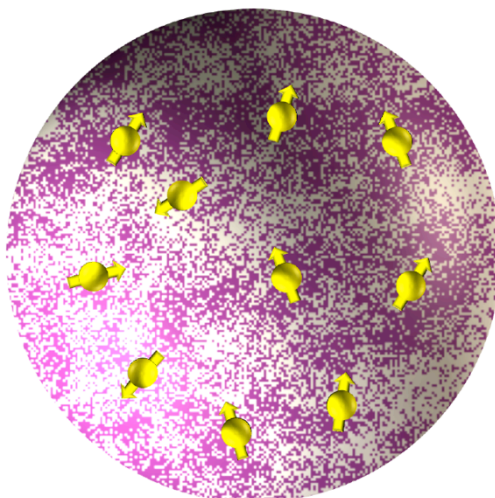
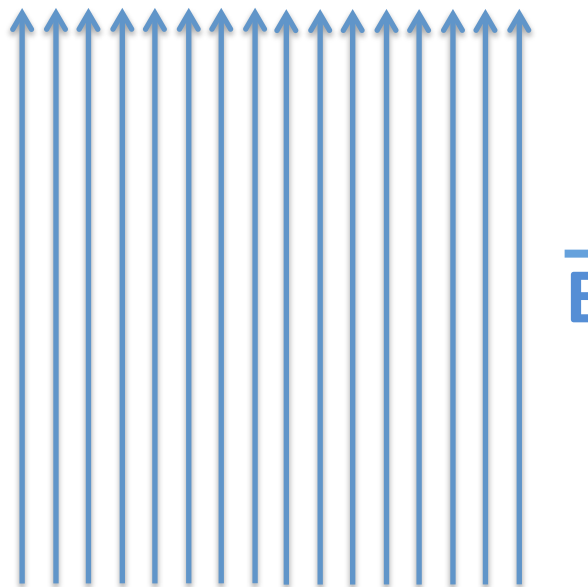
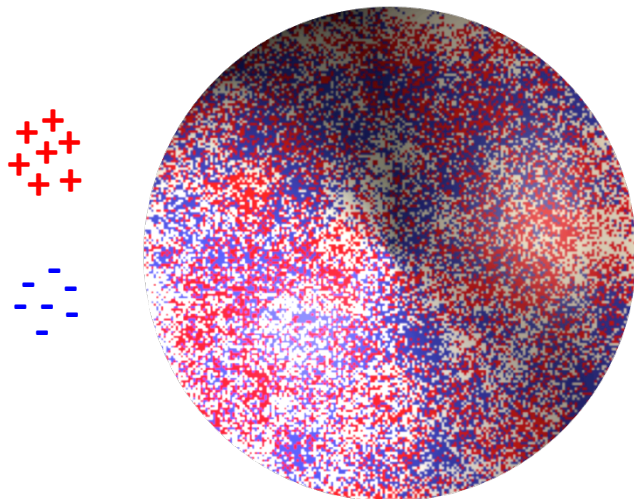
| | $P_{LT}^\perp \text{ (GeV}^{-2}\text{)}$ |
|---------------------------------|--|
| This experiment | $-15.4 \pm 3.3_{\text{(stat.)}}^{+1.5}_{-2.4} \text{ (syst.)}$ |
| DR model [16] | $-3.7 \text{ (a) , } -8.7 \text{ (b) , } -10.8 \text{ (c)}$ |
| HBCChPT $\mathcal{O}(p^3)$ [17] | -10.6 |

PRC 92 (2015) 054307

Beam-recoil polarization measurement at $Q^2=0.33 \text{ (GeV/c)}^2$

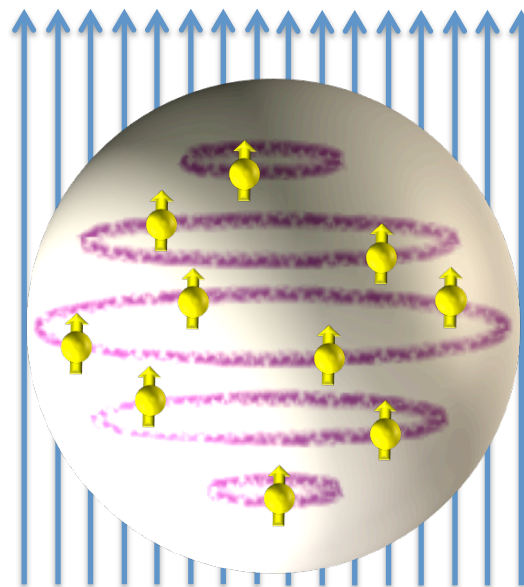
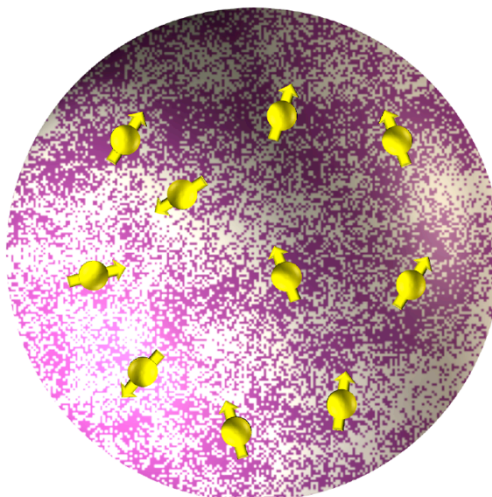
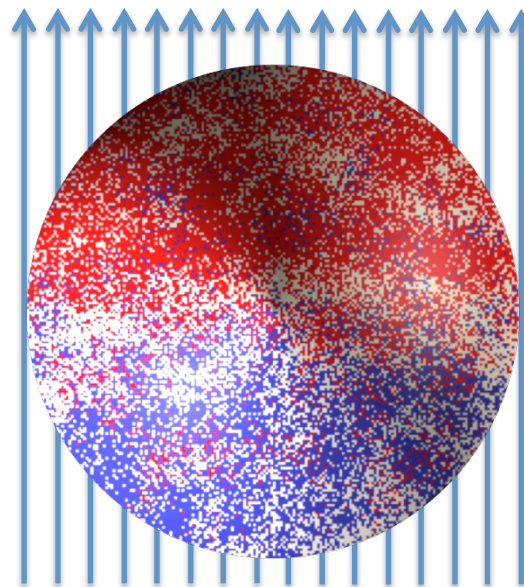
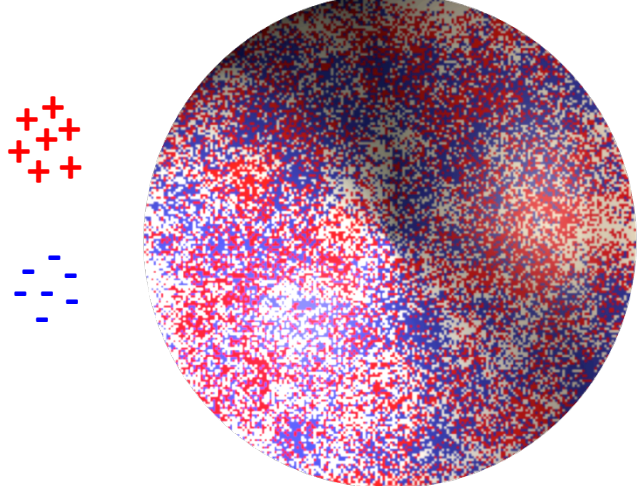
Scalar Polarizabilities

Response of internal structure to an applied EM field



Scalar Polarizabilities

Response of internal structure to an applied EM field



"stretchability"

$$\vec{d}_{\text{E induced}} \sim \alpha \vec{E}$$

External field deforms
the charge distribution

"alignability"

$$\vec{d}_{\text{M induced}} \sim \beta \vec{B}$$

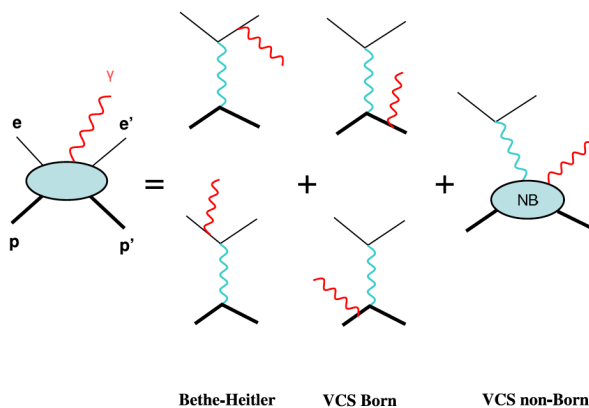
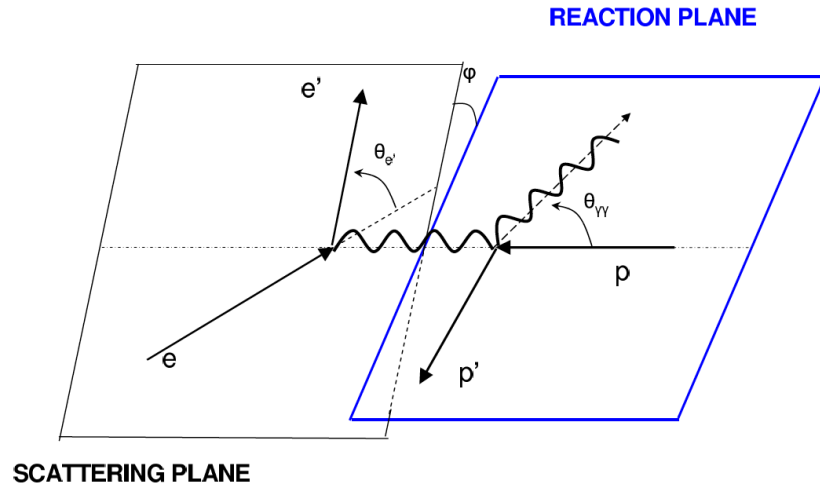
$$\beta_{\text{para}} > 0$$

$$\beta_{\text{diam}} < 0$$

Paramagnetic: proton spin aligns
with the external magnetic field

Diamagnetic: π -cloud induction produces
field counter to the external one

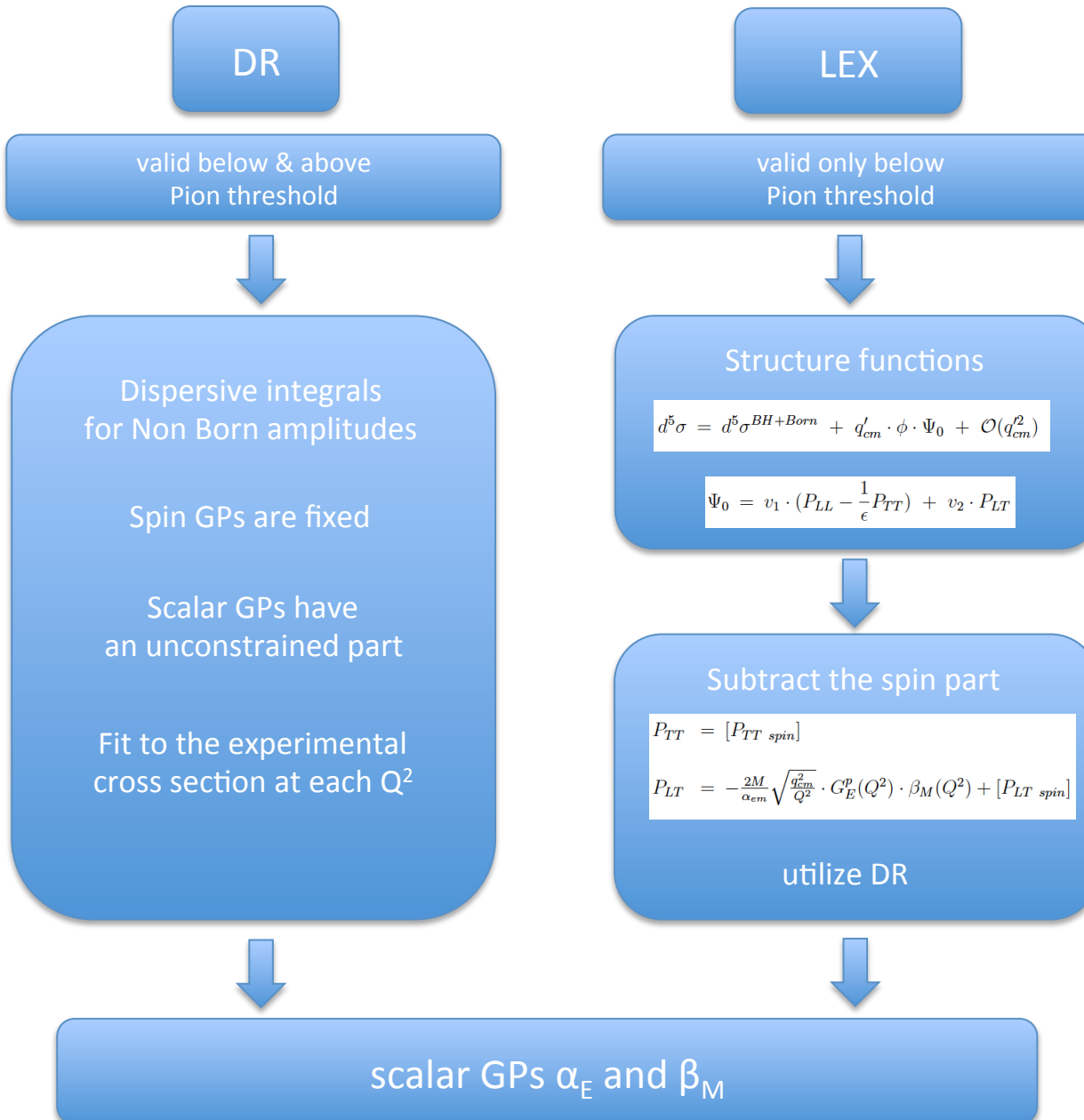
Virtual Compton Scattering



Elastic FFs

GPs

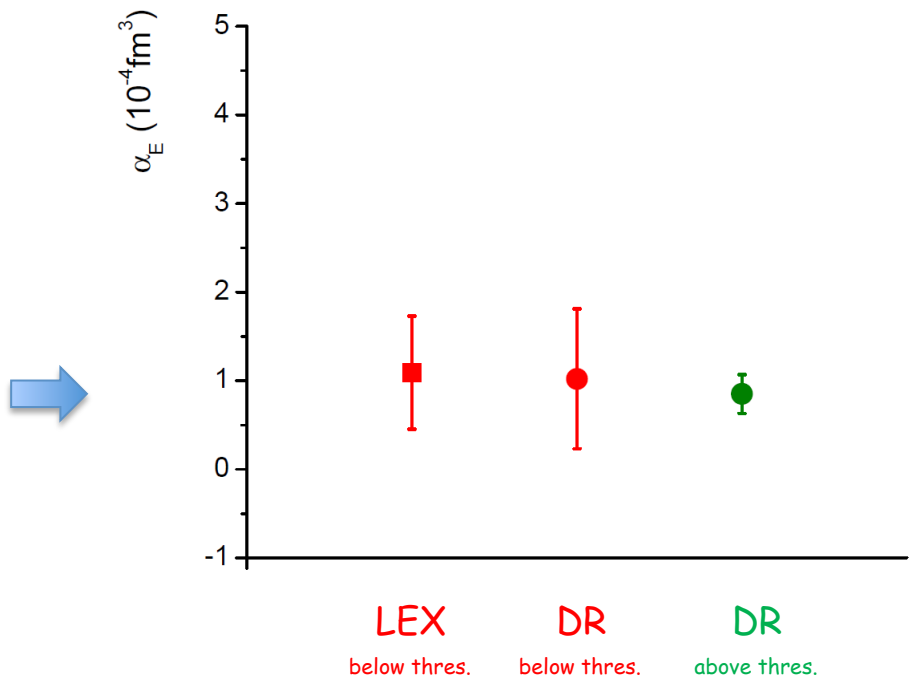
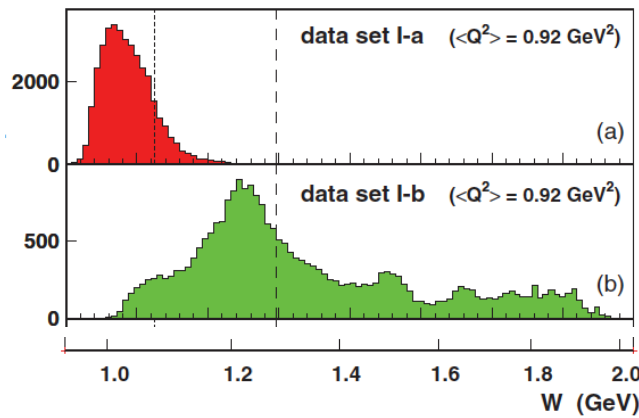
Virtual Compton Scattering



Virtual Compton Scattering

Phys. Rev C 86, 015210 (2012)

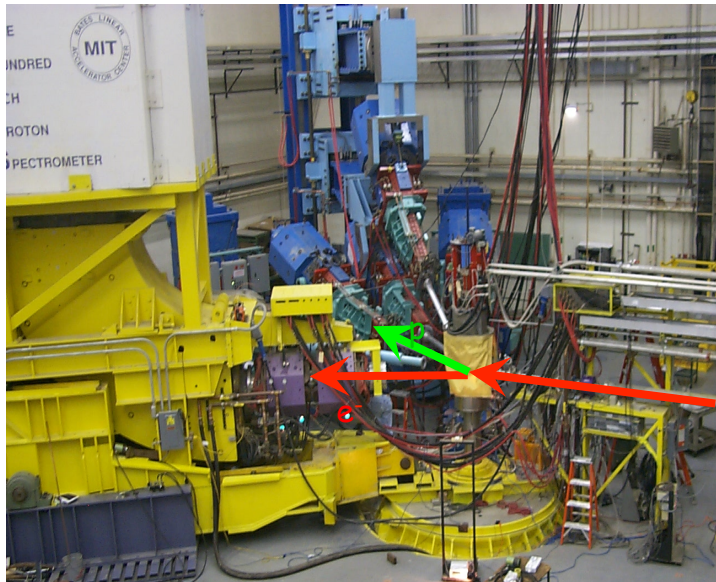
Phys. Rev Lett. 93, 122001 (2004)



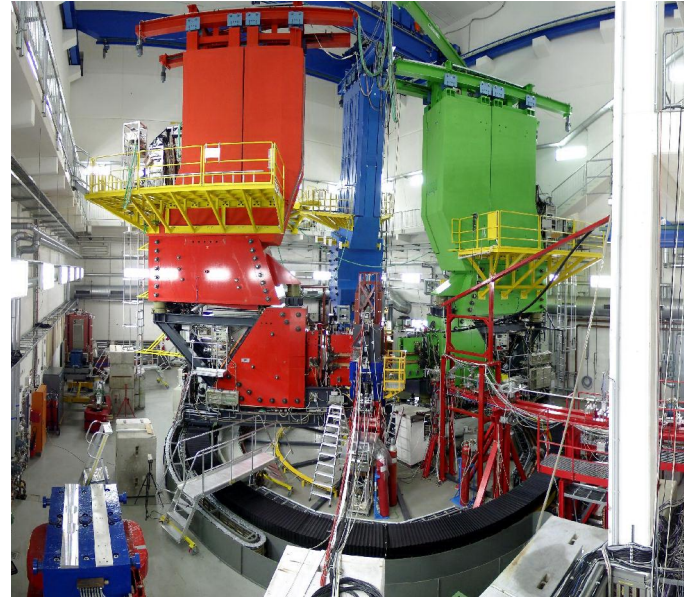
Sensitivity to the GPs grows with the photon energy

Early Experiments

MIT-Bates @ $Q^2=0.06 \text{ GeV}^2$



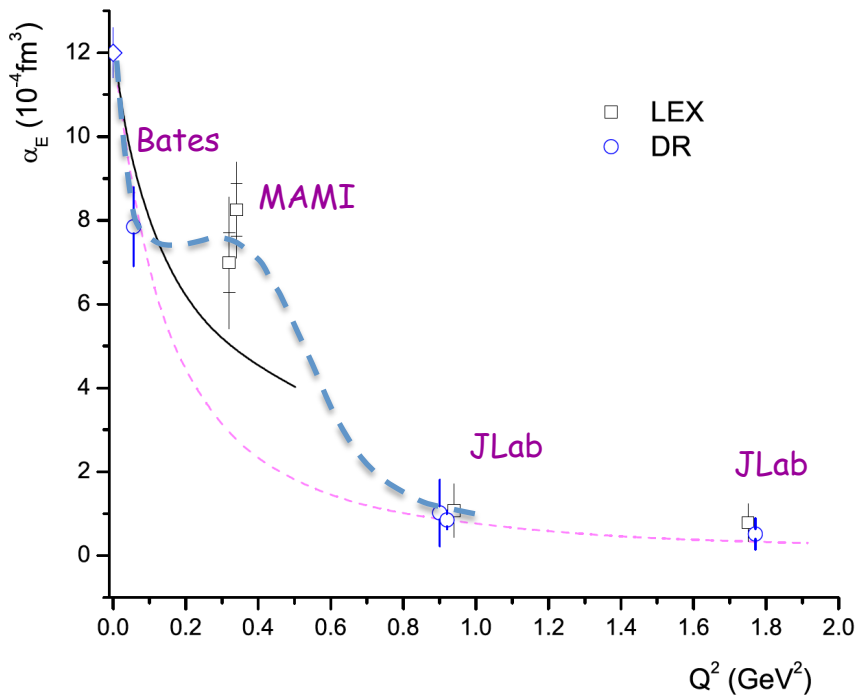
MAMI-A1 @ $Q^2=0.33 \text{ GeV}^2$



Jlab-Hall A @ $Q^2=0.9 \text{ & } 1.8 \text{ GeV}^2$



Early Experiments



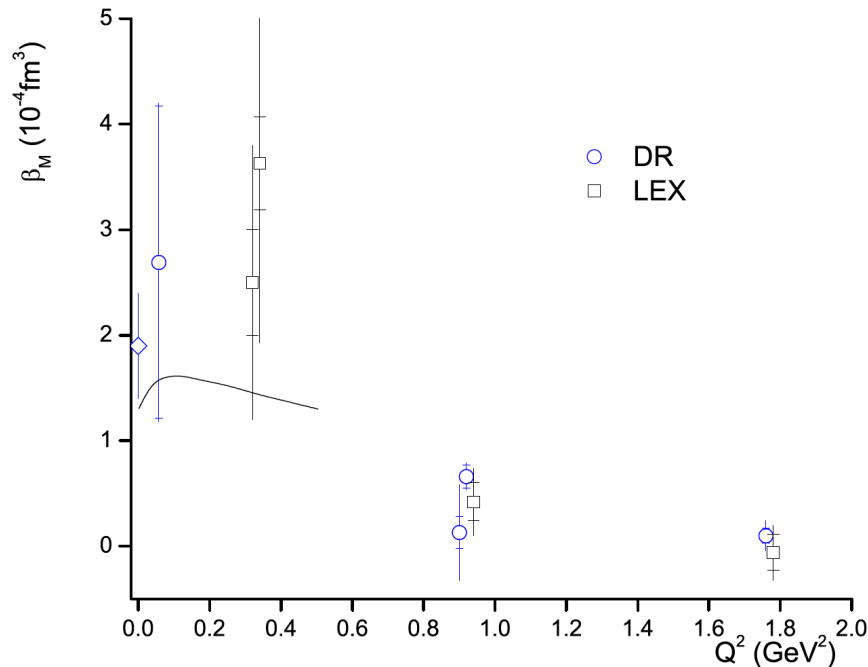
$\alpha_E \approx 10^{-3} V_N$ (stiffness / relativistic character)

Data suggest non-trivial Q^2 evolution of α_E

Current theoretical calculations not able to describe the enhancement at low Q^2

$Q^2 = 0.33 (\text{GeV}/c)^2$ measured twice at MAMI:

- Phys. Rev. Lett 85, 708 (2000)
- Eur. Phys. J. A37, 1-8 (2008)



β_M small \leftrightarrow cancellation of competing mechanisms

Large uncertainties

Higher precision measurements needed

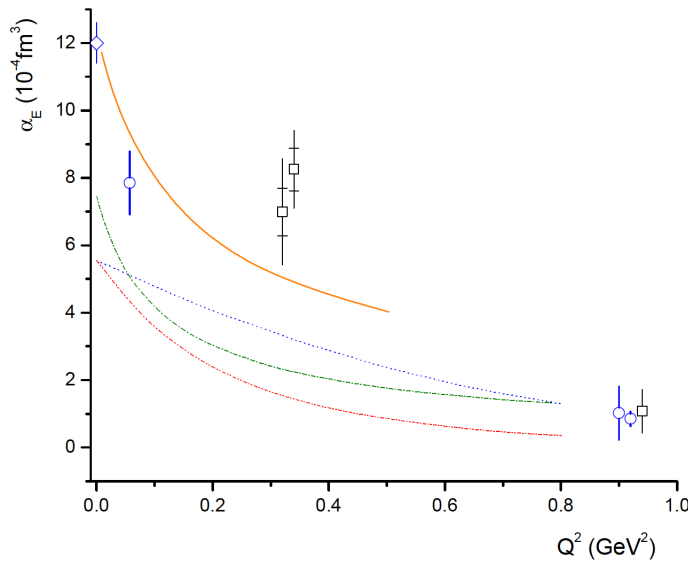
\rightarrow Quantify the balance between diamagnetism and paramagnetism

Current situation unsatisfactory:

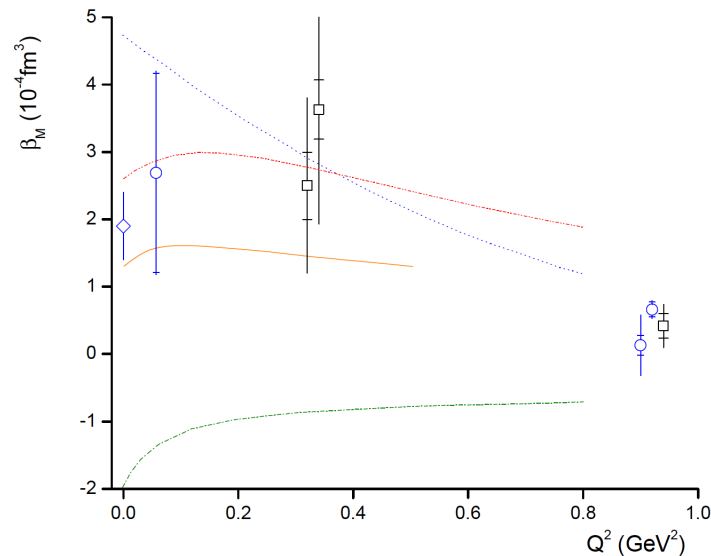
- more measurements needed (vs Q^2)
- Higher precision measurements needed

Theoretical Landscape

HBChPT
 NRQCM
 Effective Lagrangian Model
 Linear Sigma Model



| | |
|--------------------------------|--------------------------------|
| T.R. Hemmert et al | Phys. Rev. D 62, 014013 (2000) |
| B. Pasquini et al | Phys. Rev. C 63, 025205 (2001) |
| A. Yu. Korchin and O. Scholten | Phys. Rev. C 58, 1098 (1998) |
| A. Metz and D. Drechsel | Z. Phys. A 356, 351 (1996) |



All theoretical calculations predict a smooth fall off for α_E

None of the models can account for the non trivial structure of α_E suggested by the data

Lattice QCD

Currently:

Near Future:

$Q^2=0$ calculations exist but at unphysical quark masses
 calculations at the physical point for $Q^2=0$
 first calculations for $Q^2 \neq 0$

Spatial dependence of induced polarizations on an external EM field

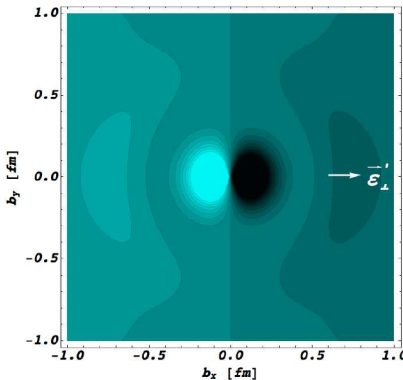
Nucleon form factor data → light-front quark charge densities

Formalism extended to the deformation of these quark densities when applying an external e.m. field:

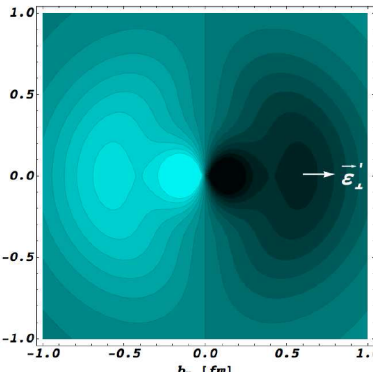
GPs → spatial deformation of charge & magnetization densities under an applied e.m. field

Induced polarization in a proton when submitted to an e.m. field

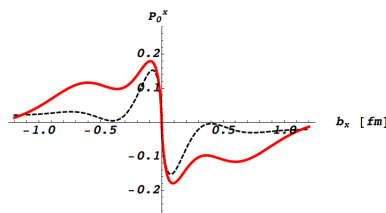
GP I



GP II



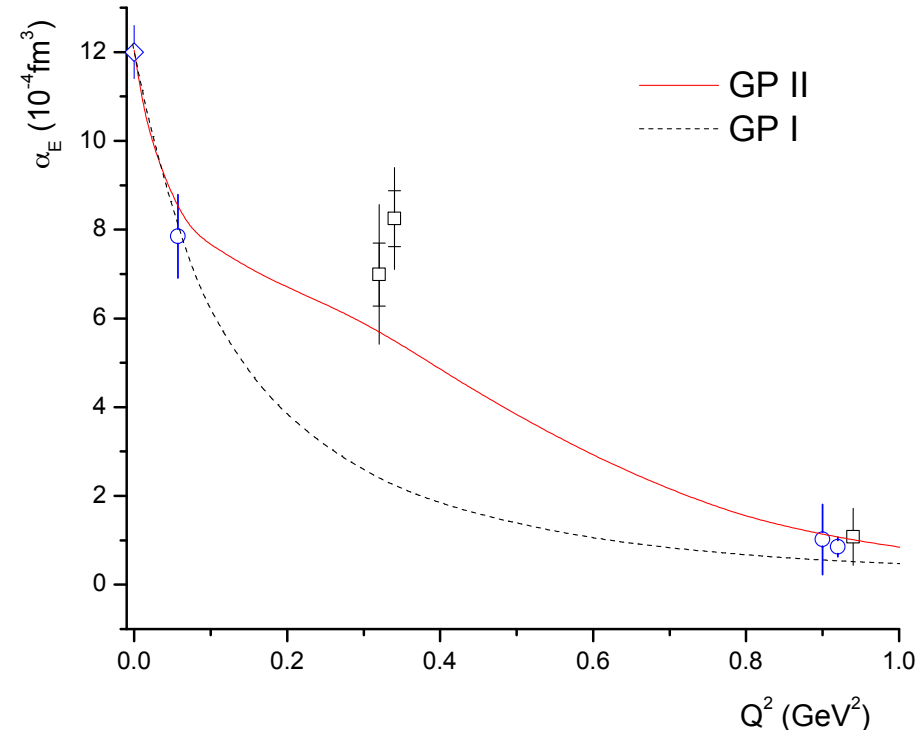
Light (dark) regions → largest (smallest) values
(photon polarization along x-axis, as indicated)



Induced polarization along $b_y = 0$

Phys. Rev. Lett. 104, 112001 (2010)

M. Gorchtein, C. Lorce, B. Pasquini, M. Vanderhaeghen



Ongoing Experimental Efforts

MAMI

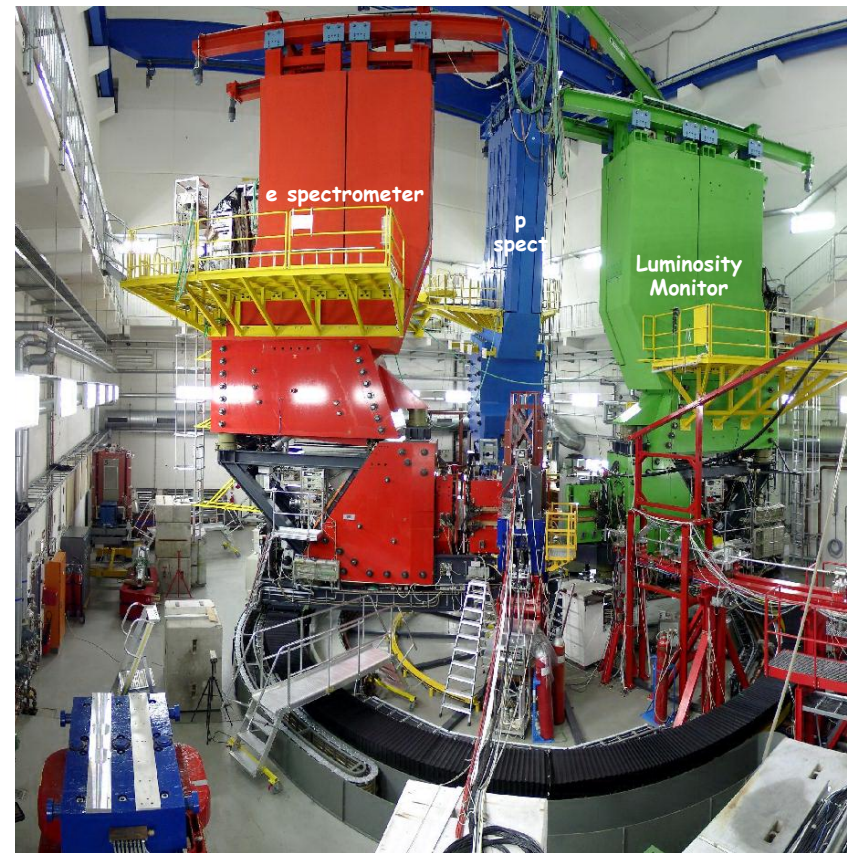
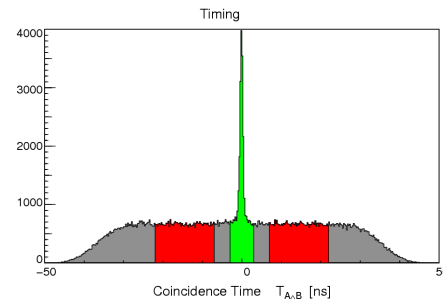
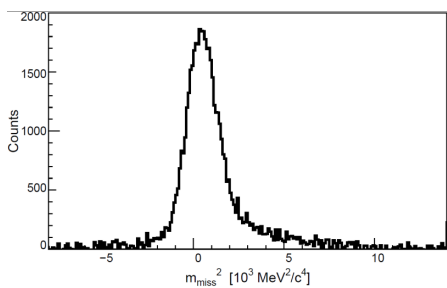
MAMI A1/1-09 (vcsq2) below threshold

MAMI A1/3-12 (vcsdelta) above threshold

Both experiments utilized
the A1 setup at MAMI

Preliminary results were
recently released

Analysis is ongoing



vcsq2 @ MAMI

$\sim 1.0 \text{ GeV beam}$

$Q^2 = 0.1 (\text{GeV}/c)^2, 0.2 (\text{GeV}/c)^2, \text{ and } 0.45 (\text{GeV}/c)^2$

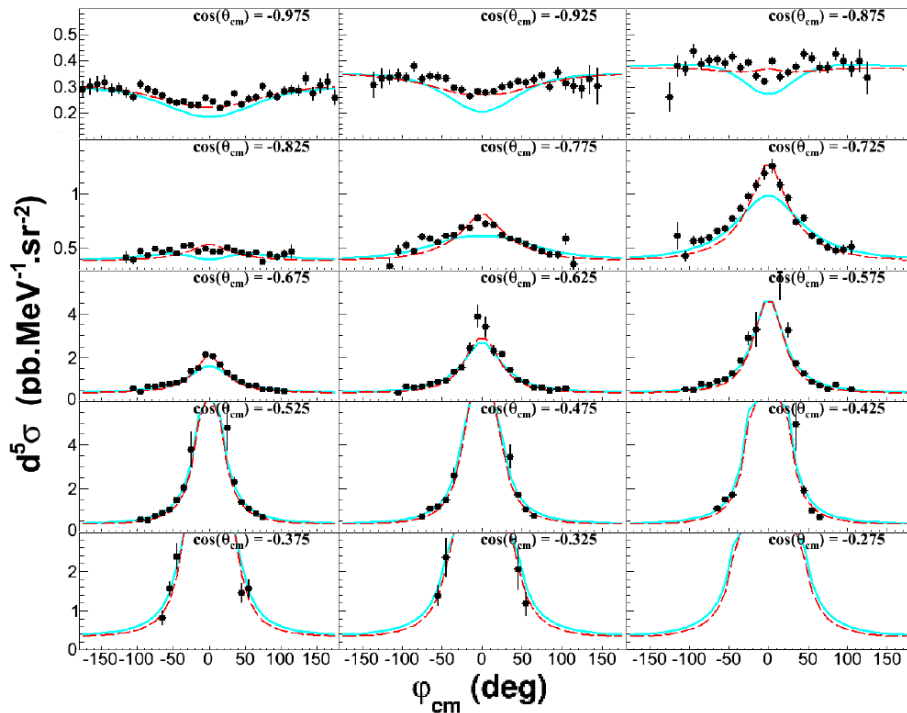


Figure 5.8: Setting INP: measured $ep \rightarrow e\gamma$ cross section at fixed $q'_{cm} = 112.5 \text{ MeV}/c$ with respect to φ_{cm} for all the $\cos(\theta_{cm})$ -bins. The curves follow the convention of figure 5.6.

Figure from PhD thesis of L. Correa, Mainz / Cl. Ferrand, 2016

BH+B ---
Polarizability ---
effect

GP effect typically 0 - 15%
of the cross section

Polarizability fits:

DR fit:

DR calculation includes full dependency in q'_{cm}

LEX fit:

truncated in q'_{cm} . Suppress contribution
from higher order terms

For LEX the higher order terms have to be negligible

$$d^5\sigma = d^5\sigma^{BH+Born} + q'_{cm} \cdot \phi \cdot \Psi_0 + \mathcal{O}(q'^2_{cm})$$

A phase space masking has to be applied to keep these terms smaller than the 2%-3% level

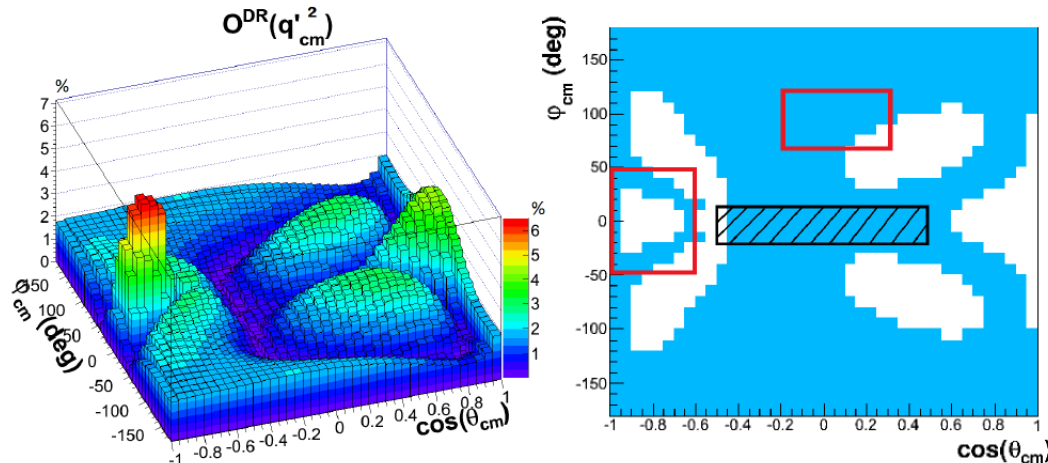
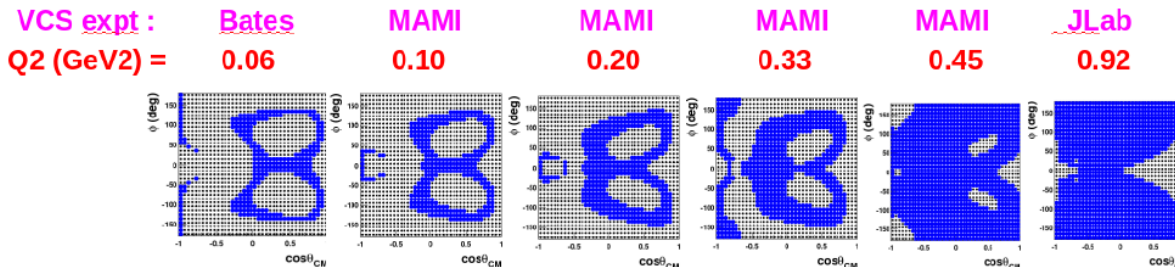
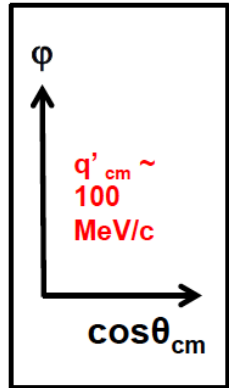


Figure 3.13: (Left) behavior of $\mathcal{O}^{DR}(q'_{cm})^2$ in the $(\cos(\theta_{cm}), \varphi_{cm})$ -plane at $q'_{cm} = 87.5 \text{ MeV}/c$ and (right) two-dimensional representation of the angular region where $\mathcal{O}^{DR}(q'_{cm})^2 < 2\%$ (blue), the red squares correspond to the two areas of interest to perform the GP extraction.

Figure from PhD thesis of L. Correa, Mainz / Cl. Ferrand, 2016

**Blue bins = where the higher-order estimator is < 3%
(LEX truncation « valid »)**



New « vcsq2 » data:

- OOP kinematics (to access the blue region)
- LEX Fit done with bin selection at $Q^2 = 0.1$ and 0.2 GeV^2 .
- was found not necessary at $Q^2 = 0.45 \text{ GeV}^2$.



In-plane



8.5 deg OOP

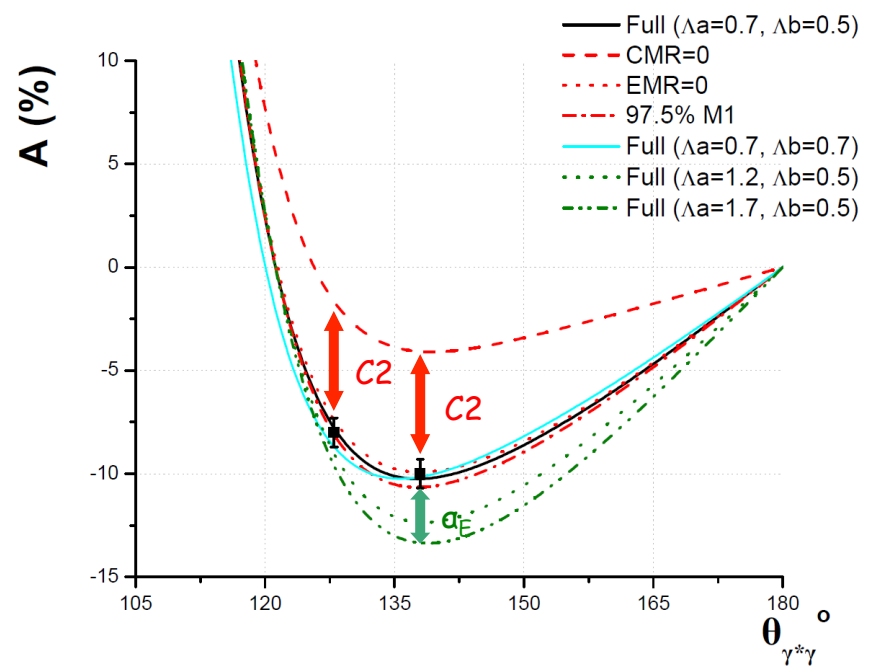
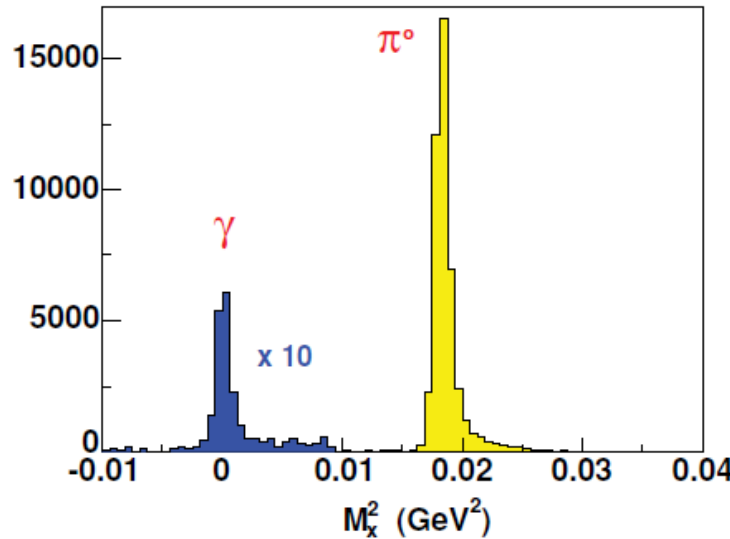
vcsdelta @ MAMI

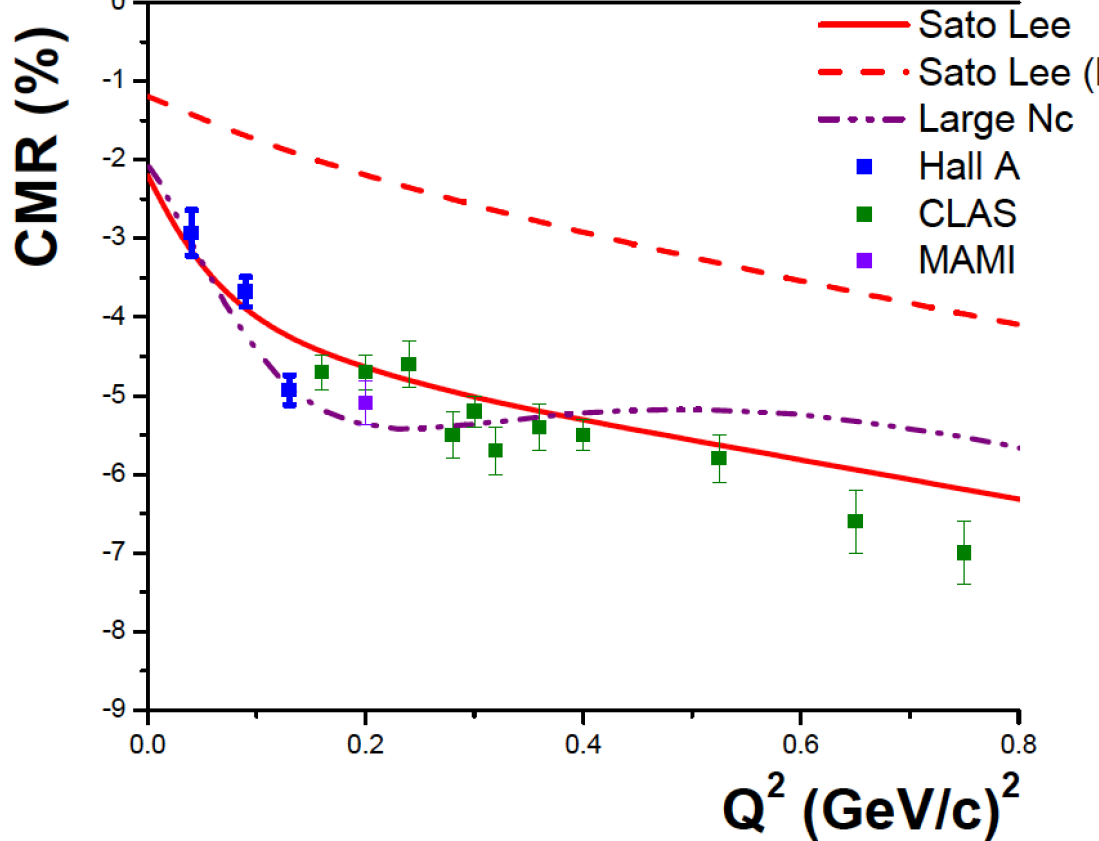
Goal 2-fold:

- 1) Measurement of the electric GP α_E
- 2) First measurement of $N \rightarrow \Delta$ transition form factors through the γ channel

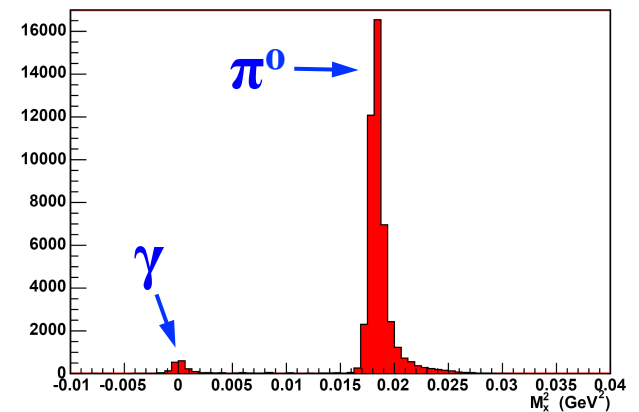
1.1 GeV beam

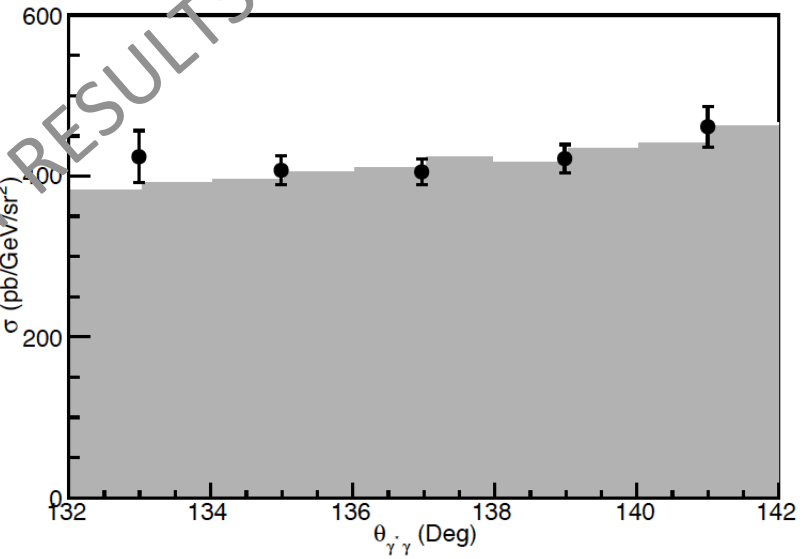
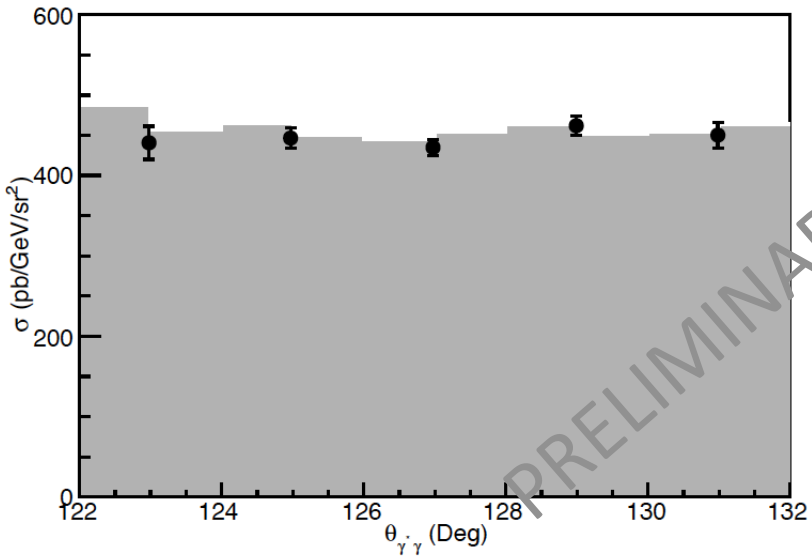
Measurement at $Q^2 = 0.2 (\text{GeV}/c)^2$

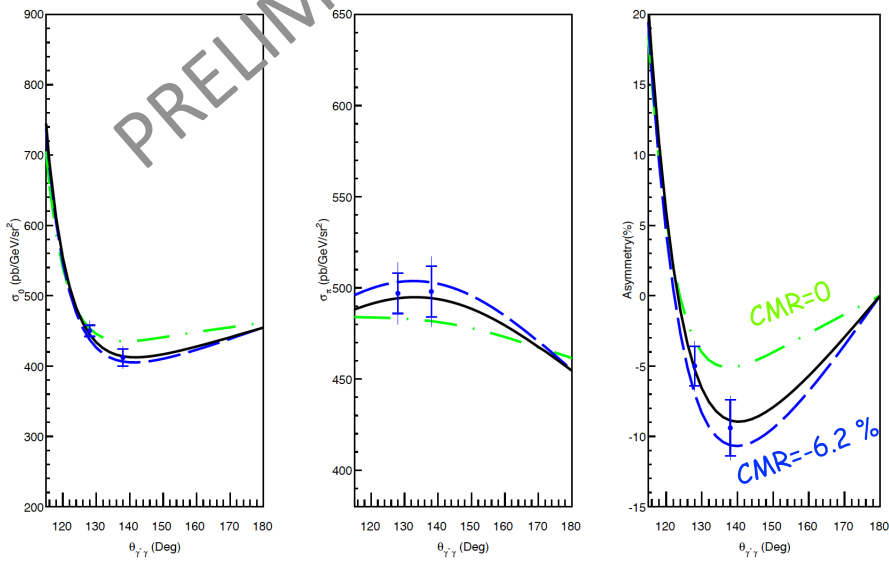
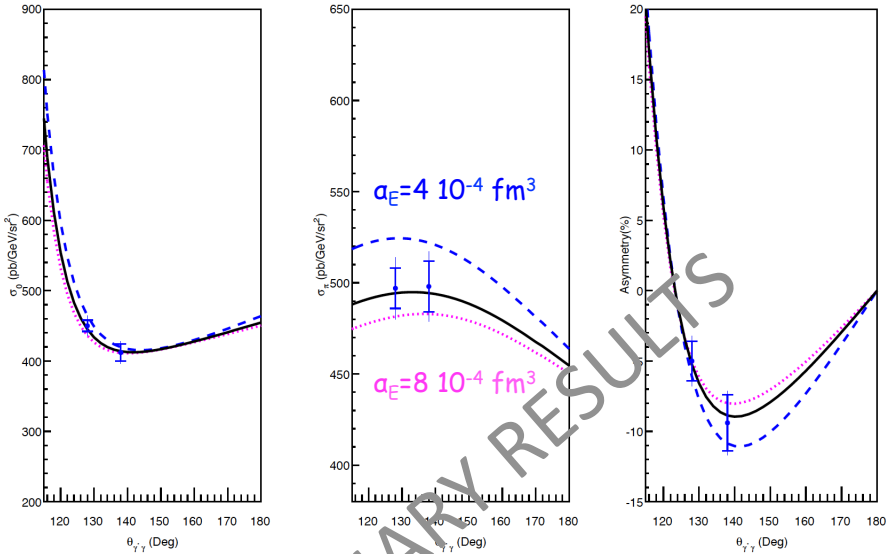




| | |
|---------------------|-----------------|
| $H(e, e' p) \pi^0$ | $\approx 66\%$ |
| $H(e, e' \pi^+) n$ | $\approx 33\%$ |
| $H(e, e' p) \gamma$ | $\approx 0.6\%$ |



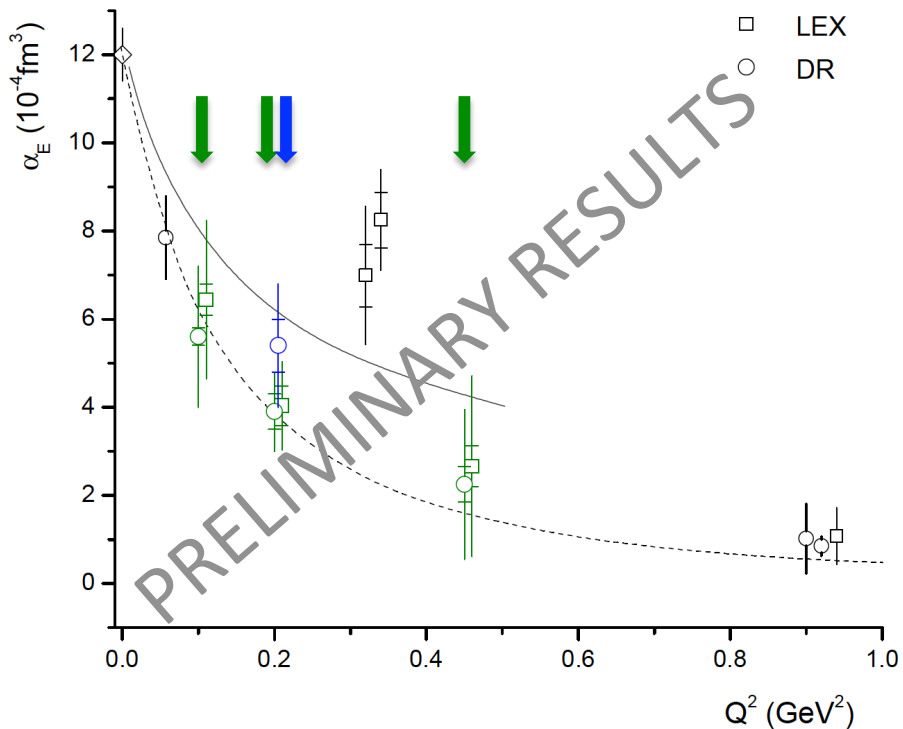




MAMI Preliminary Results

Preliminary A1/1-09 (vcsq2)

Preliminary A1/3-12 (vcsdelta)



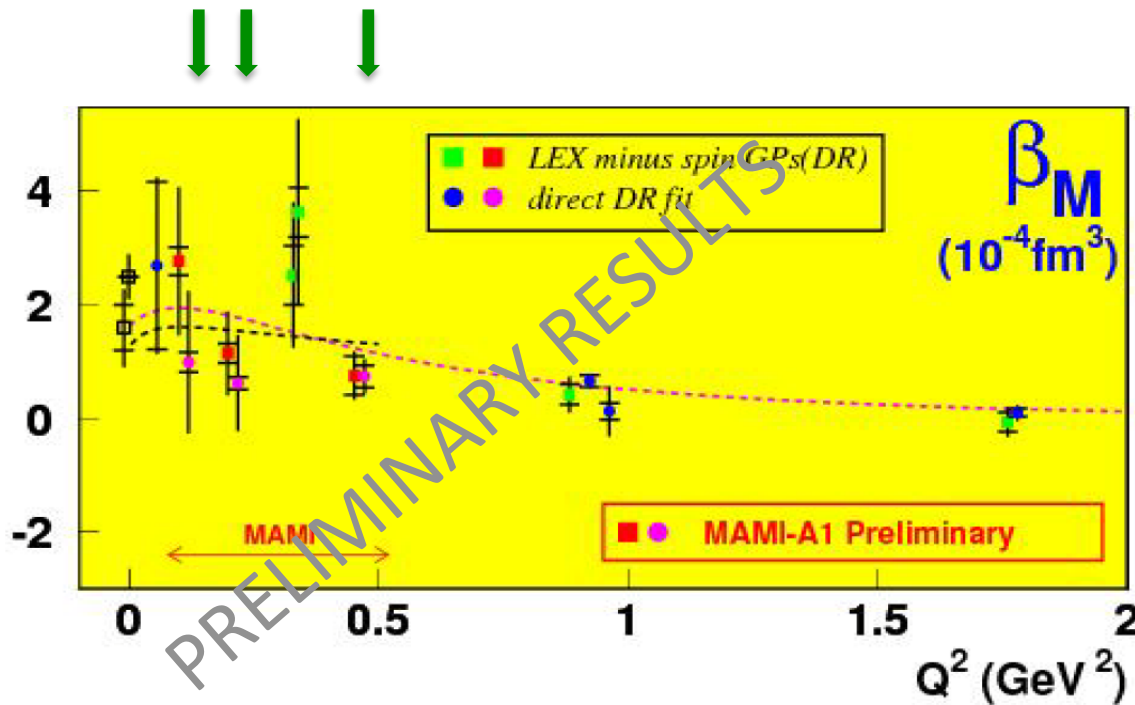
Data analyzed by 4 PhD students

Jure Bericic (Ljubljana Univ.)
Loup Correa (Clermont-Fd Univ.)
Meriem BenAli (Clermont-Fd Univ.)
Adam Blomberg (Temple Univ.)

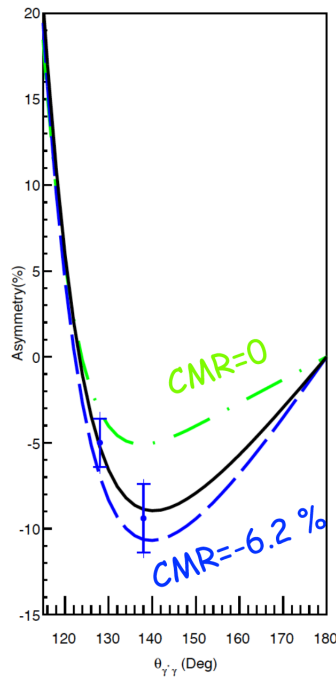
2 independent measurements at $Q^2=0.20 \text{ (GeV/c)}^2$

MAMI Preliminary Results

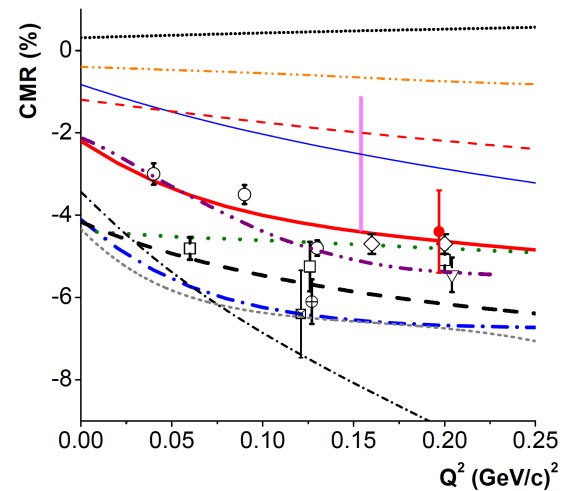
Preliminary A1/1-09 (vcsq2)



MAMI Preliminary Results



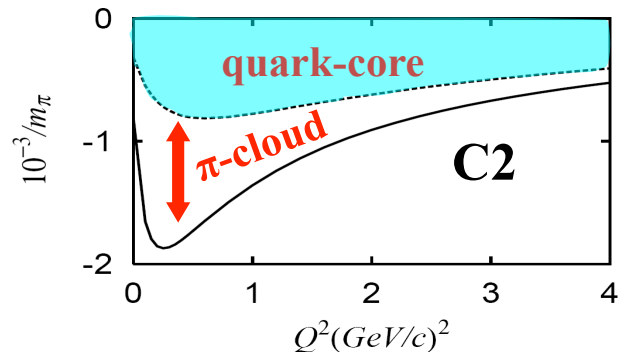
| | | |
|--------------------|---------------------|---------------|
| ● photon channel | — MAID | — PV |
| ○ Hall A | — DMT | — GH |
| □ MAMI | — Sato Lee | — HQM |
| ◇ CLAS | - - Sato Lee (bare) | — Capstick |
| ⊕ Bates | • SAID | — Lattice QCD |
| ▽ Elsner et al | — Large-Nc | |
| ☒ Pospischil et al | — DSEM | |



First measurement of the N- Δ C2 amplitude through the photon channel

Important for cross check to the world data and for cross checking & constraining the model uncertainties

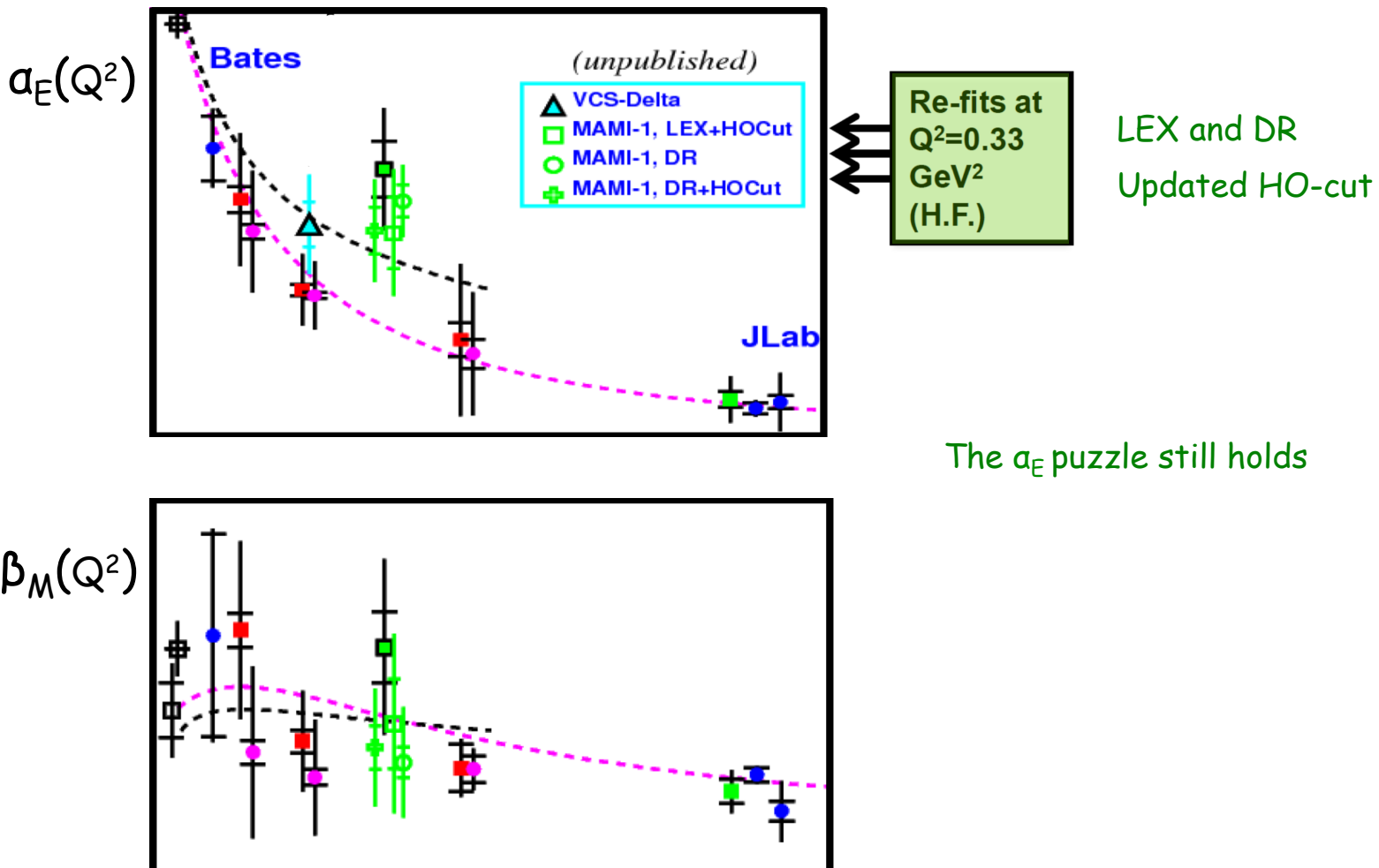
Sato Lee
Phys. Rev. C 54, 2660 (1996)
Phys. Rev. C 63, 055201 (2001)



Revisiting the $Q^2=0.33 \text{ GeV}^2$ data

$Q^2 = 0.33 \text{ (GeV}/c)^2$ measured twice at MAMI - two different experiments

- Phys. Rev. Lett 85, 708 (2000)
- Eur. Phys. J. A37, 1-8 (2008)



Ongoing Experimental Efforts

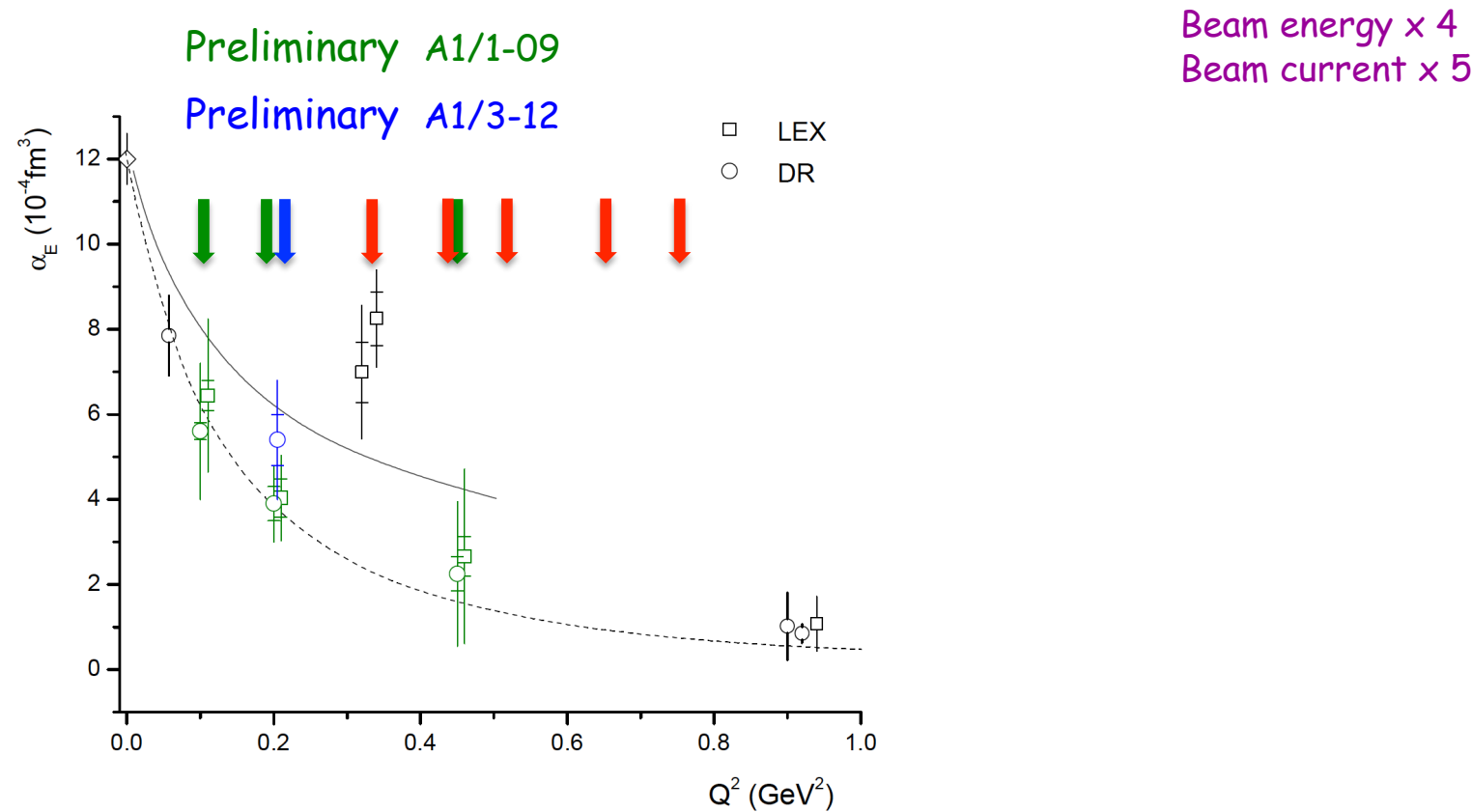
JLab

New Experiment

E12-15-001
(JLab)

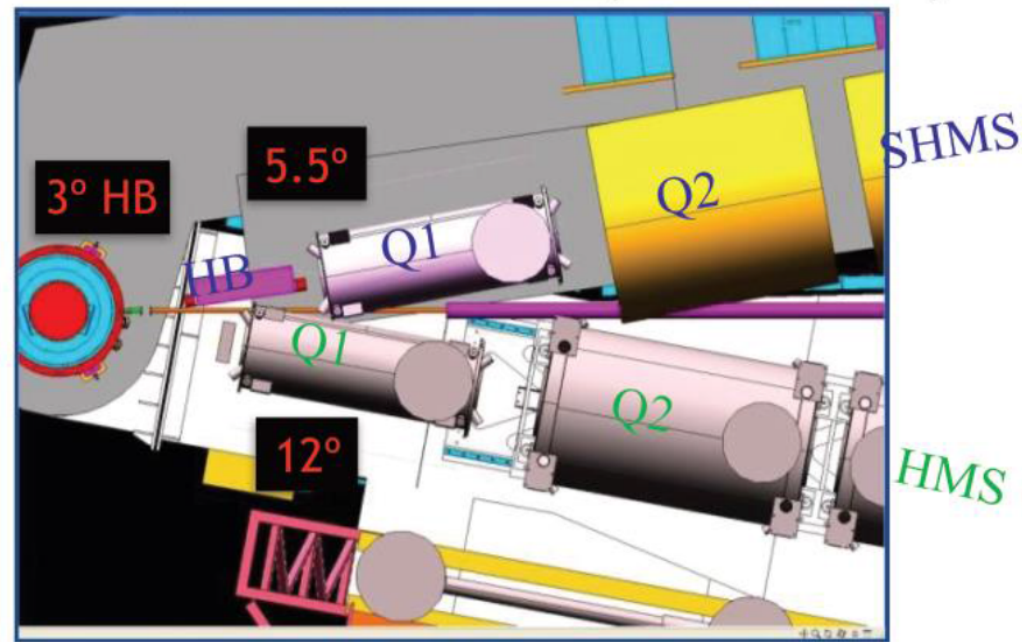
Going from $\epsilon = 0.6 \rightarrow 0.9$ doubles the sensitivity to the GPs

$\epsilon=0.97$ (Jlab)
 $\epsilon=0.62$ (MAMI)



JLab Hall C with 12 GeV upgrade

- Super High Momentum Spectrometer
 - HB, 3 Quads, Dipole
 - $P \rightarrow 2 - 11 \text{ GeV}$
 - Resolution: $\delta < 0.1\%$
 - Acceptance: $\delta \rightarrow 30\%$, 4 msr
 - $5.5^\circ < \theta < 40^\circ$
 - Good e/ π /K/p PID
- High Momentum Spectrometer
 - 3 Quads, Dipole
 - $P \rightarrow 7.5 \text{ GeV}$
 - Resolution: $\delta < 0.1\%$
 - Acceptance: $\delta \rightarrow 18\%$, 6.5 msr
 - $10.5^\circ < \theta < 90^\circ$
 - Good e/ π /K/p PID
- Minimum opening angle $\sim 17^\circ$
- Well shielded detector huts
- 2 beam line polarimeters
- Ideal facility for:
 - Rosenbluth (L/T) separations
 - Exclusive reactions
 - Low cross sections (neutrino level)



Slide Courtesy
of S. Wood

Hall C HMS and SHMS

SHMS:

- 11-GeV Spectrometer
- Partner of existing 6-GeV HMS

MAGNETIC OPTICS:

- Point-to Point QQD for easy calibration and wide acceptance.
- Horizontal bend magnet allows acceptance at forward angles (5.5°)

Detector Package:

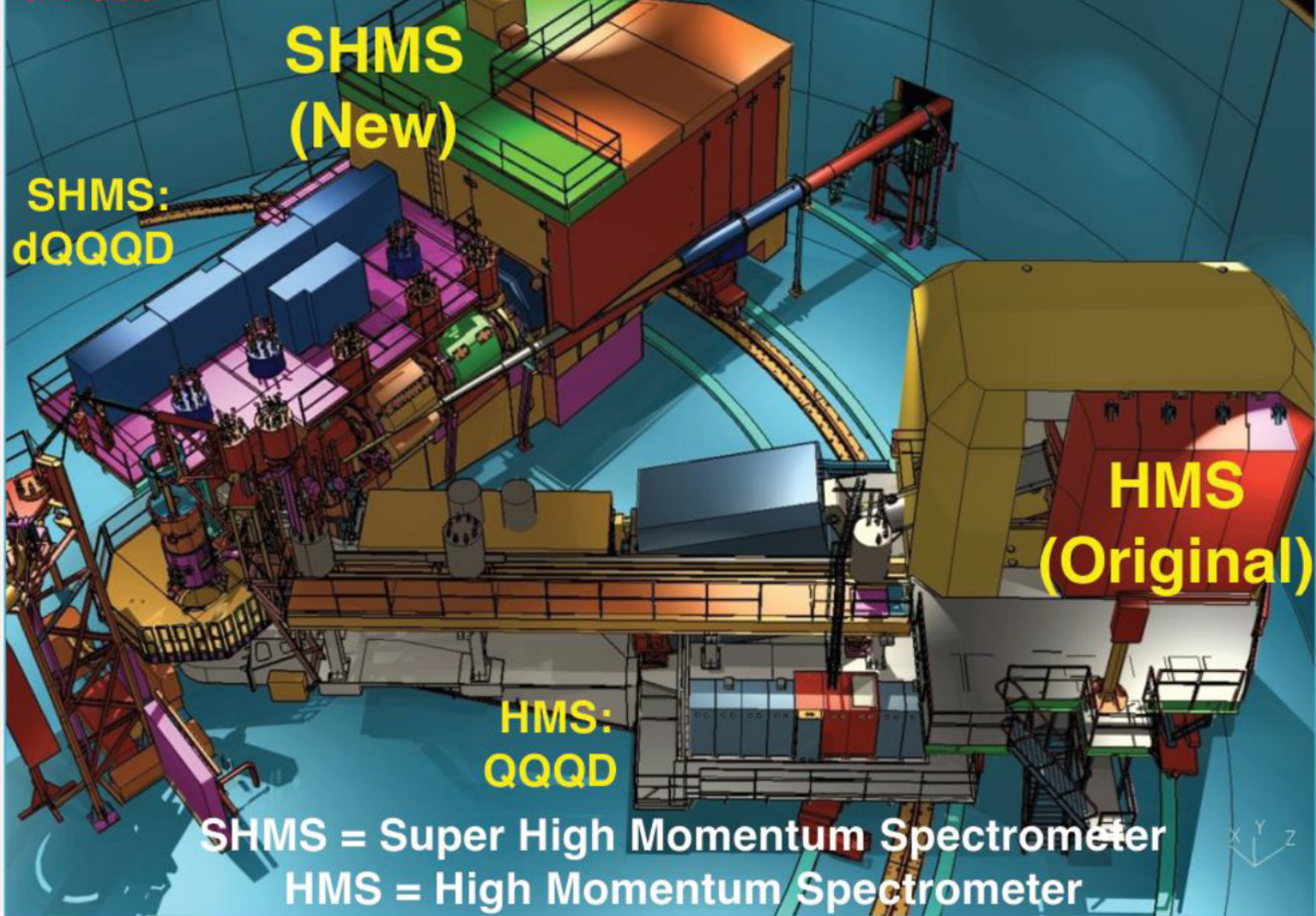
- Drift Chambers
- Hodoscopes
- Cerenkovs
- Calorimeter
- All derived from existing HMS/SOS detector designs

Well-Shielded Detector Enclosure

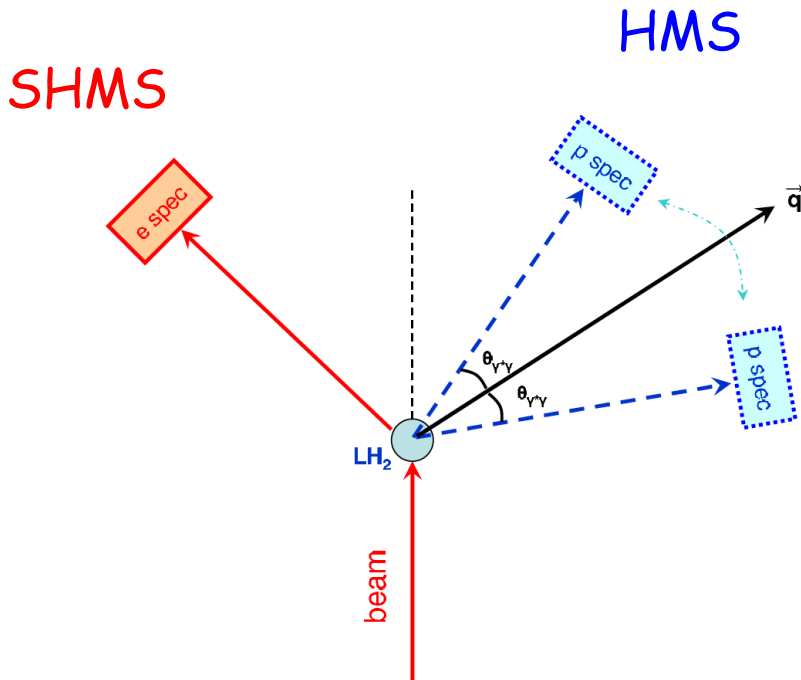
Rigid Support Structure

- Rapid & Remote Rotation
- Provides Pointing Accuracy & Reproducibility demonstrated in HMS

Slide Courtesy
of H. Feneker



E12-15-001 Experimental Setup



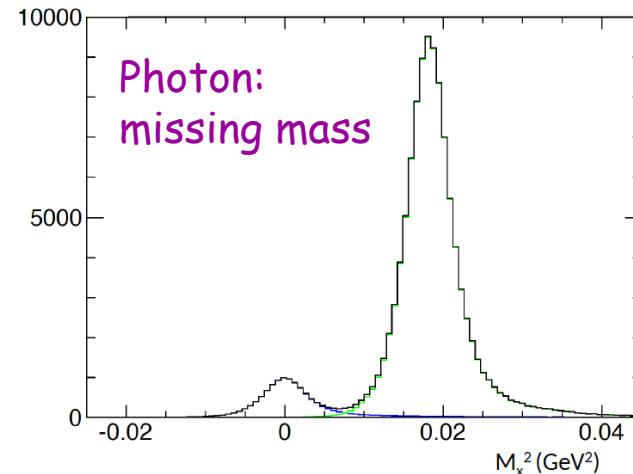
Hall C: SHMS, HMS

4.4 GeV

40-85 μ A

Liquid hydrogen 15 cm

e & p detection in coincidence



cross sections

in-plane azimuthal asymmetries

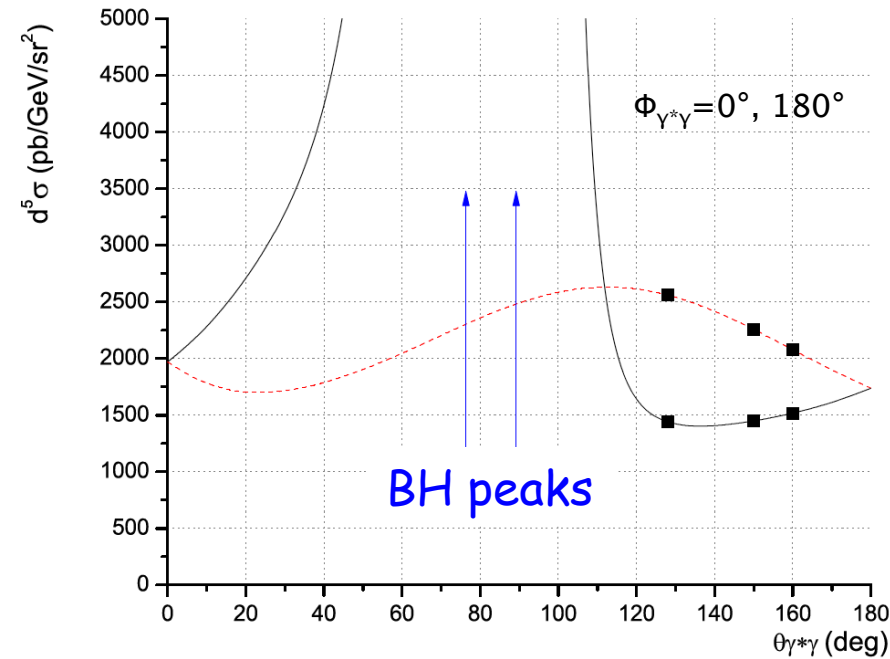
$$A_{(\phi_{\gamma^*\gamma}=0,\pi)} = \frac{\sigma_{\phi_{\gamma^*\gamma}=0} - \sigma_{\phi_{\gamma^*\gamma}=180}}{\sigma_{\phi_{\gamma^*\gamma}=0} + \sigma_{\phi_{\gamma^*\gamma}=180}}$$

sensitivity to GPs

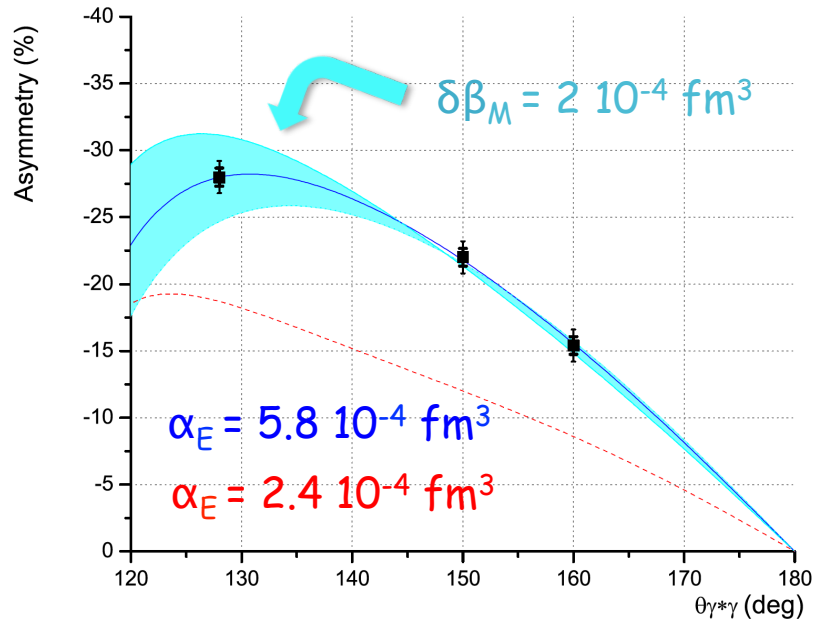
suppression of systematic uncertainties

Projected Measurements

$$Q^2 = 0.43 \text{ (GeV/c)}^2$$



avoid BH peaks
stay at $\theta_{\gamma^*\gamma} > 120^\circ$



Kinematical Settings

| | Kinematical Setting | $\theta_{\gamma^*\gamma} \circ$ | $\theta_e \circ$ | $P'_e(MeV/c)$ | $\theta_p \circ$ | $P'_p(MeV/c)$ | S/N | beam time (days) |
|---------|---------------------|---------------------------------|------------------|---------------|------------------|---------------|-----|------------------|
| Part I | Kin Ia | 155 | 7.97 | 3884.4 | 37.20 | 893.20 | 1.1 | 0.5 |
| | Kin Ib | 155 | 7.97 | 3884.4 | 51.26 | 893.20 | 2.7 | 0.5 |
| | Kin IIa | 140 | 7.97 | 3884.4 | 33.08 | 859.90 | 1 | 0.45 |
| | Kin IIb | 140 | 7.97 | 3884.4 | 55.38 | 859.90 | 3.7 | 0.55 |
| | Kin IIIa | 120 | 7.97 | 3884.4 | 27.85 | 794.68 | 0.9 | 0.45 |
| | Kin IIIb | 120 | 7.97 | 3884.4 | 60.61 | 794.68 | 6.2 | 0.55 |
| | Kin IVa | 165 | 9.39 | 3820.5 | 40.85 | 1010.40 | 1.3 | 0.5 |
| | Kin IVb | 165 | 9.39 | 3820.5 | 48.45 | 1010.40 | 2.4 | 0.5 |
| | Kin Va | 155 | 9.39 | 3820.5 | 38.34 | 995.20 | 1 | 0.5 |
| | Kin Vb | 155 | 9.39 | 3820.5 | 50.96 | 995.20 | 3.2 | 0.5 |
| Part II | Kin VIa | 128 | 9.39 | 3820.5 | 31.84 | 919.43 | 0.7 | 0.95 |
| | Kin VIb | 128 | 9.39 | 3820.5 | 57.46 | 919.43 | 7.8 | 0.55 |
| | Kin VIIa | 165 | 11.54 | 3708.6 | 40.81 | 1175.25 | 2.6 | 1.5 |
| | Kin VIIb | 165 | 11.54 | 3708.6 | 47.35 | 1175.25 | 5 | 2 |
| | Kin VIIIa | 160 | 11.54 | 3708.6 | 39.73 | 1167.72 | 2.2 | 1.5 |
| | Kin VIIIb | 160 | 11.54 | 3708.6 | 48.43 | 1167.72 | 6.3 | 2 |
| Part II | Kin IXa | 140 | 11.54 | 3708.6 | 35.52 | 1117.38 | 1.2 | 1.5 |
| | Kin IXb | 140 | 11.54 | 3708.6 | 52.64 | 1117.38 | 8 | 2 |

Part I

Part II

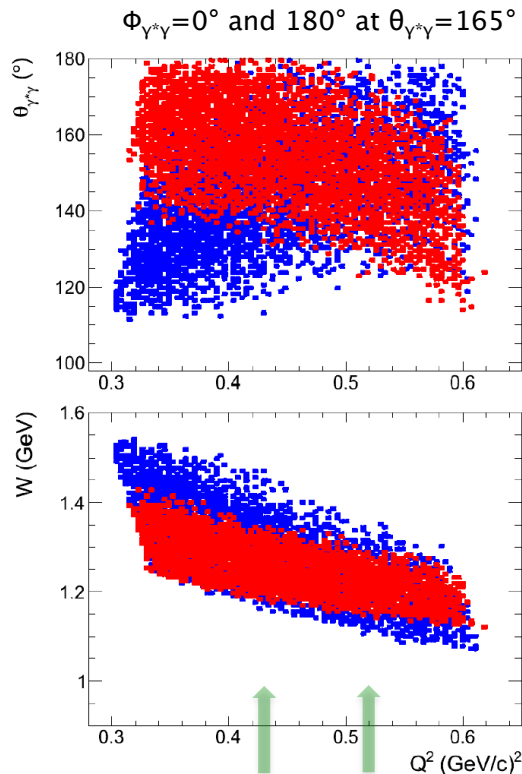
SHMS: one change of setting through Part I
same position & momentum through out Part II

Same beam energy
for all settings

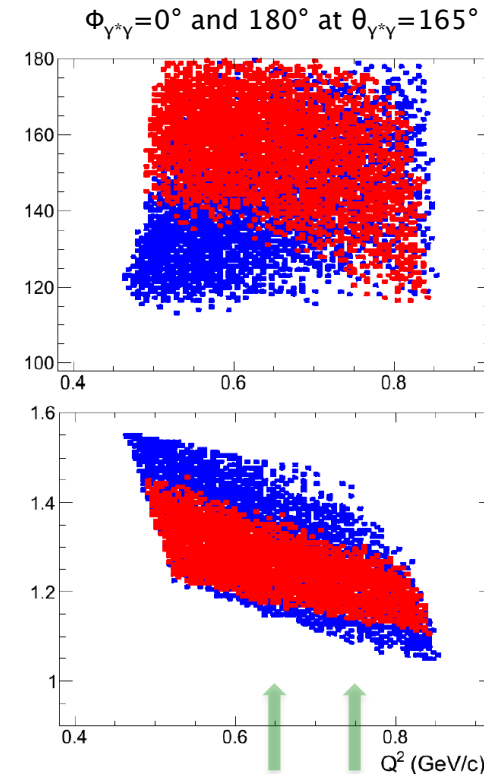
| Part | I | I | I | II | II |
|----------------|---------------------------|---------------------------|---------------------------|---------------------------|---------------------------|
| Q ² | 0.33 (GeV/c) ² | 0.43 (GeV/c) ² | 0.52 (GeV/c) ² | 0.65 (GeV/c) ² | 0.75 (GeV/c) ² |

Phase Space

Part I



Part II



Phase space binned
in Q^2 , W , $\theta_{\gamma^*\gamma}$, $\Phi_{\gamma^*\gamma}$

Cross section:
DR calculation,
B. Pasquini

Eur. Phys. J. A11 (2001) 185-208
Phys. Rept. 378 (2003) 99-205

Part

I

I

I

II

II

Q^2

0.33 (GeV/c)

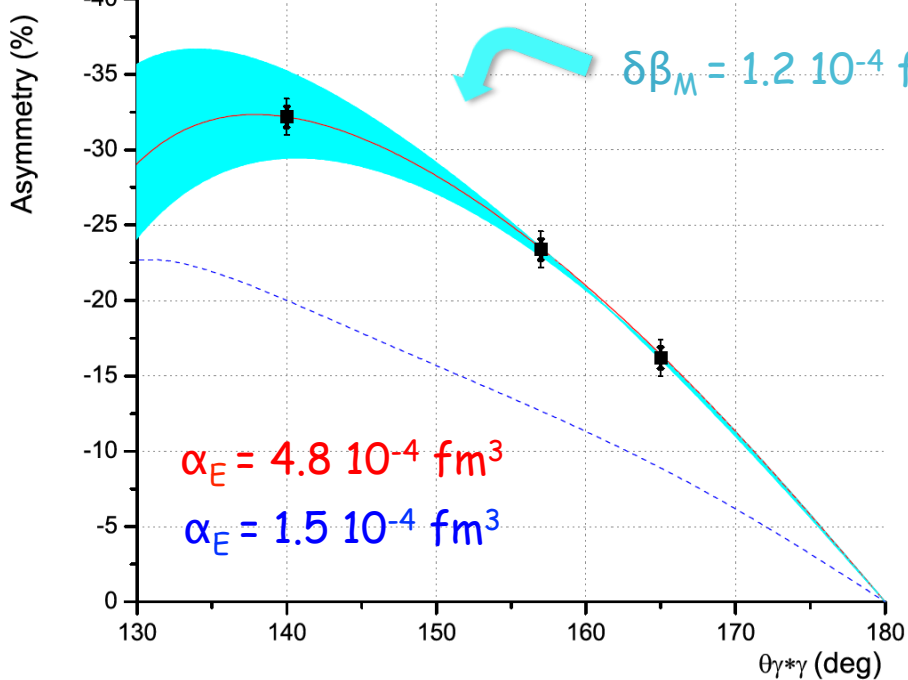
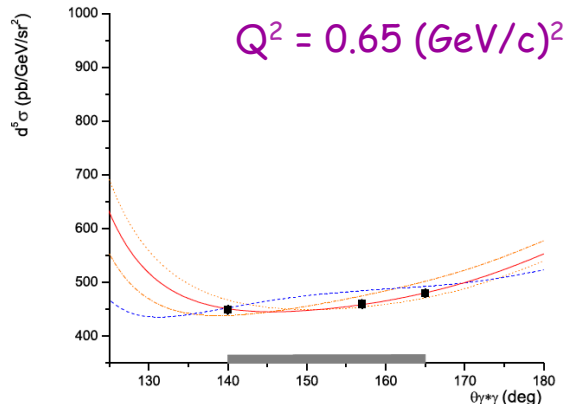
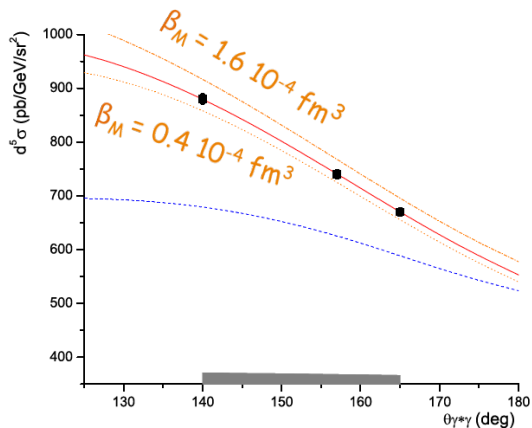
0.43 (GeV/c^2)

0.52 (GeV/c^2)

0.65 (GeV/c^2)

0.75 (GeV/c^2)

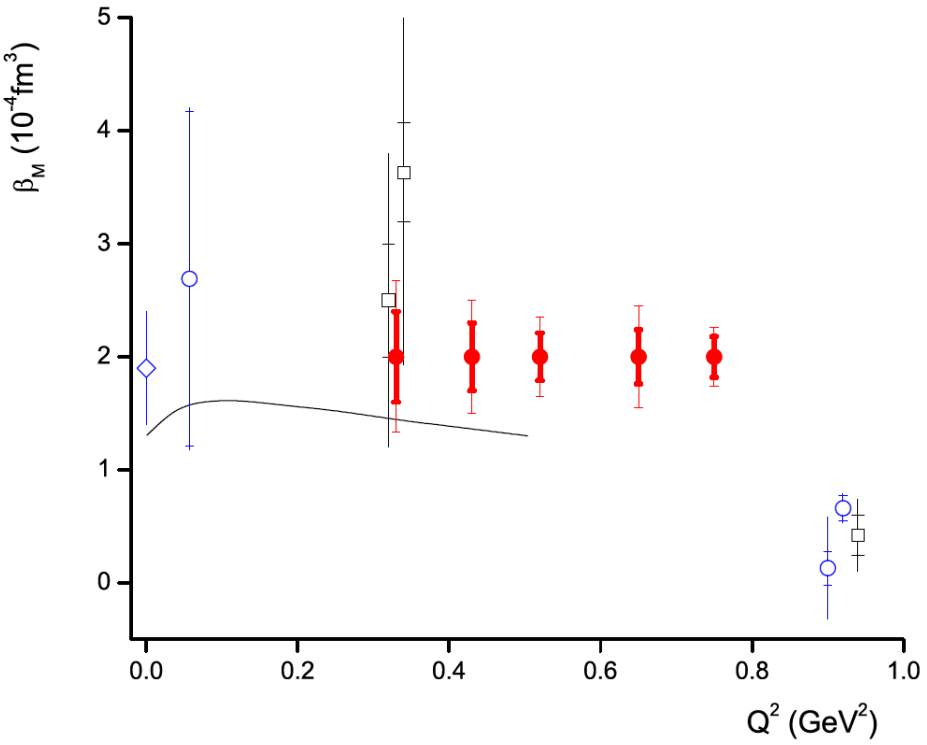
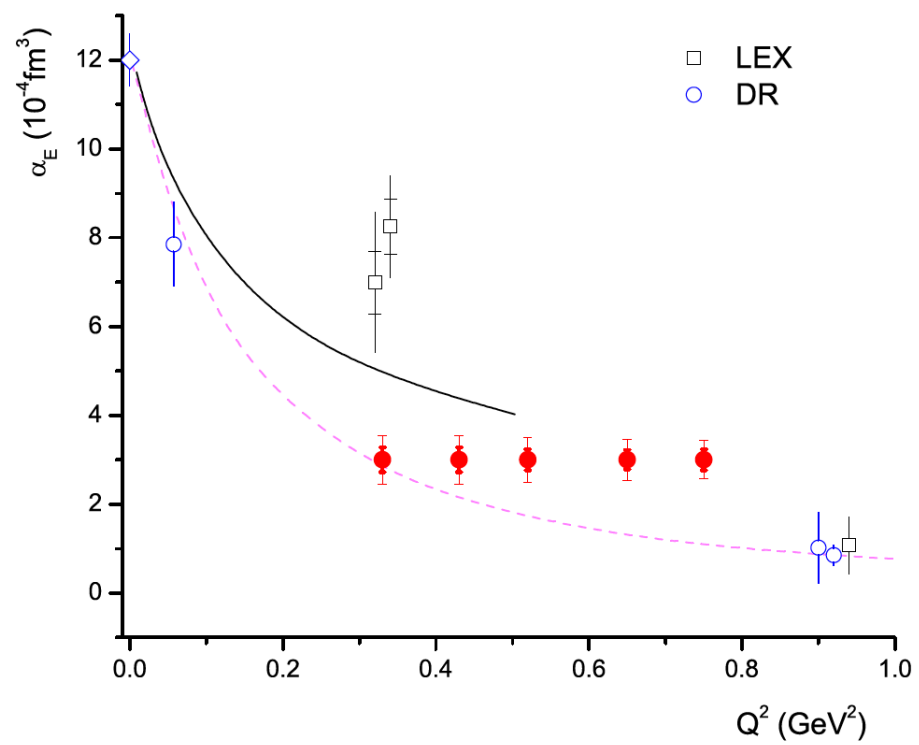
Projected Measurements



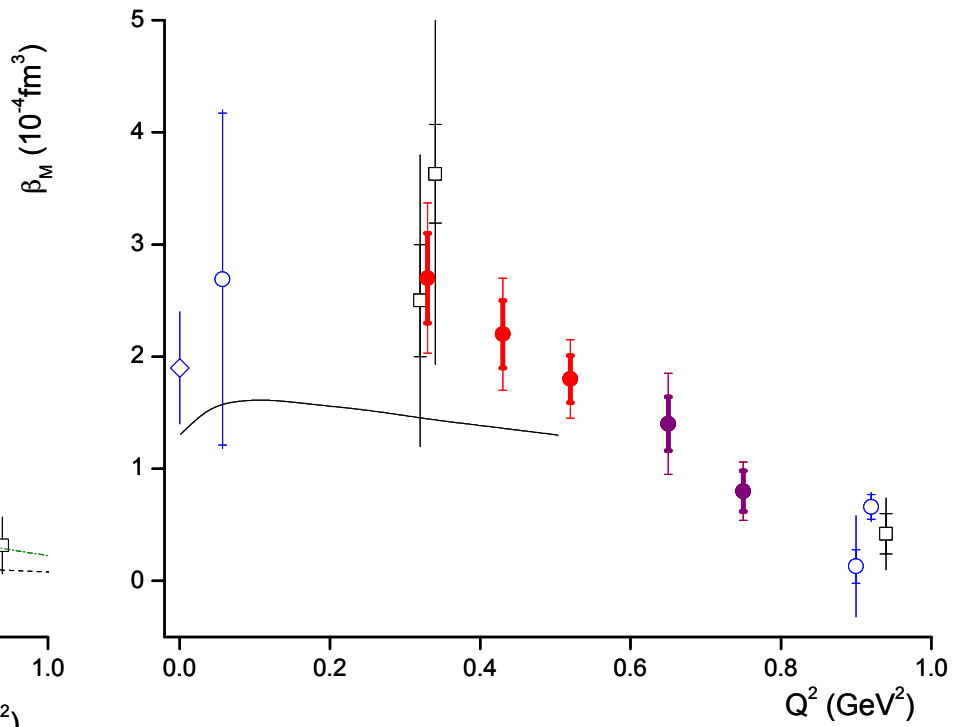
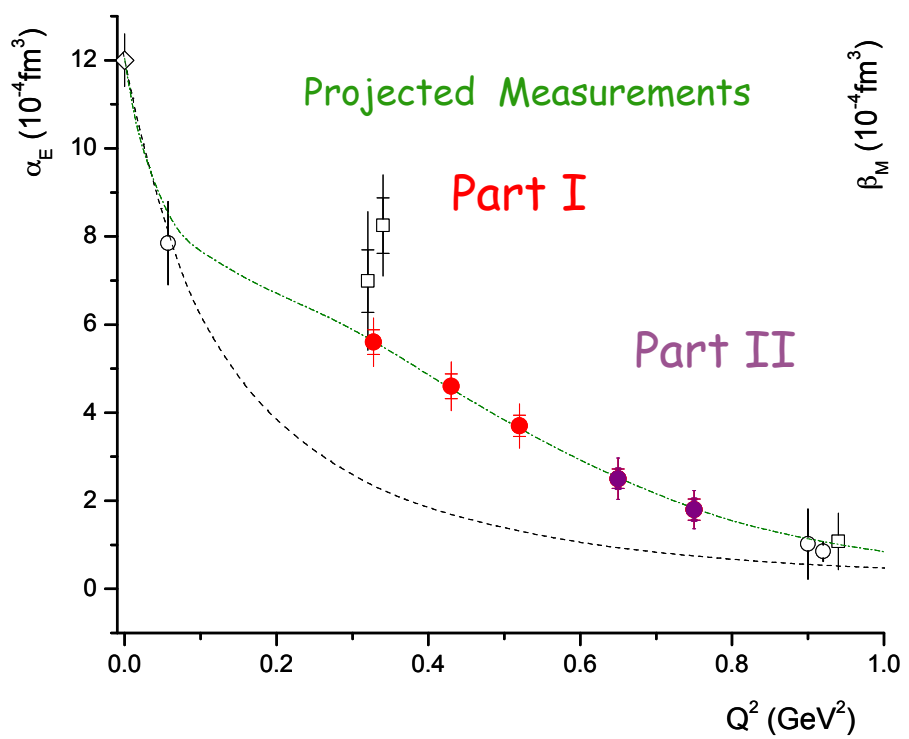
| | |
|---------------------------|---------|
| Statistical | < ±1.3% |
| Beam energy / scat. Angle | ±1-2.5% |
| Target density | ±0.5% |
| Detector efficiency | ±0.5% |
| Acceptance | ±0.5% |
| Target cell backgr. | ±0.5% |
| Target length | ±0.3% |
| Beam charge | ±0.3% |
| Dead time | ±0.3% |
| Pion contamination in MM | ±0.3% |
| Rad. Corr. | ±1.5% |
| Other | ±0.5% |

σ < ±1.3% (stat) < ±3.3% (syst)
 A ≈ ±0.7% (stat) ≈ ±1.1% (syst)

Projected Measurements



Status of E12-15-001



Part I approved in summer 2016 (Jlab PAC 44): (4.4 GeV, 85 μA , Hall C)

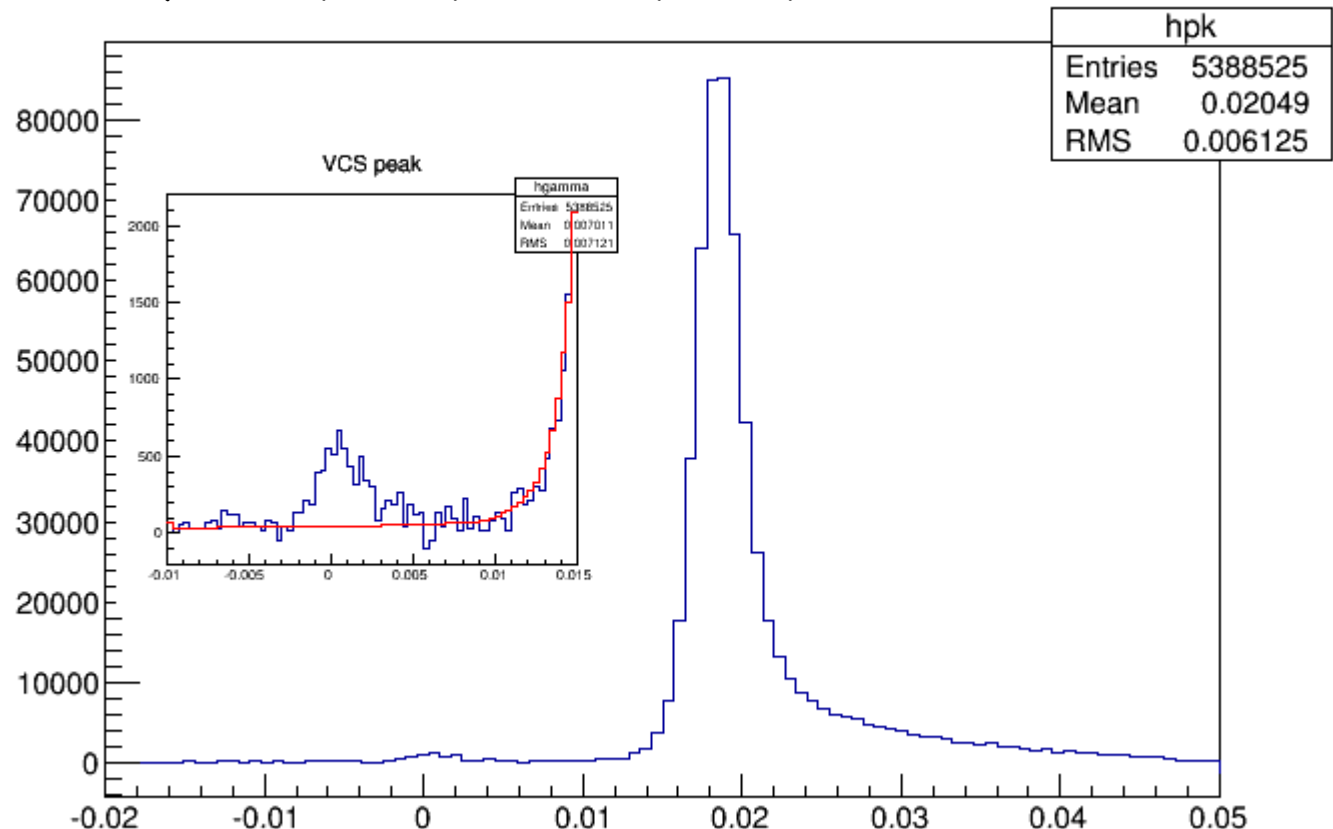
Current plan is to take data in June 2019

Other ongoing efforts

E08-010 (Hall-A/Jlab): γ -channel

parasitic access to VCS - data analysis ongoing

$Q^2 = 0.04 \text{ (GeV/c)}^2 \text{ to } 0.13 \text{ (GeV/c)}^2$



Summary

Intense experimental effort focusing on the measurement of the electric and magnetic GPs

- fundamental structure constants
- internal structure and dynamics of the nucleon
- complementary information to elastic & transition FFs, GPDs, TMDs, ...

Puzzle w.r.t. a_E

New results (MAMI) and an upcoming new experiment (Jlab)
in a region very sensitive to the nucleon dynamics

- improve the precision of a_E and β_M by a factor of 2
- GPs Q^2 signature
- explore mechanism for the non trivial Q^2 dependence of a_E
- quantify the balance between paramagnetism and diamagnetism through β_M
- provide, with high precision, the spatial deformation of charge & magnetization densities under an applied e.m. field (currently a profound structure is suggested in the region 0.5 fm - 1 fm)
- Lattice QCD results will be emerging in the next few years - very important to cross check these calculations
- the new measurements will trigger more theoretical activity

Thank you!